

Universidad Autónoma de San Luis Potosí
Facultad de Ciencias



**Study of optical properties of two-dimensional
and one-dimensional systems at the mi-
croscopic level: Polarization effects**

Thesis

To obtain the degree of

PhD. in Applied Sciences

by:

Gabriela Flores Rangel

Supervisors:

Dr. Luis Felipe Lastras Martínez

Dr. Ricardo Castro García

SAN LUIS POTOSÍ, S.L.P. MÉXICO

AUGUST 2022

STATEMENT OF AUTHORSHIP

I, Gabriela Flores Rangel, student of the Graduate Program in Applied Sciences of the Faculty of Sciences of the Universidad Autonoma de San Luis Potosi, as author of the thesis "Study of optical properties of two-dimensional and one-dimensional systems at the microscopic level: Polarization effects", declare that the thesis is an original, unpublished, authentic, personal work, that the corresponding sources have been cited and that in its execution the legal provisions in force that protect the copyright and intellectual and industrial property rights were respected. The ideas, doctrines, results and conclusions I have reached are my absolute responsibility.

ABSTRACT

In this work a structural study of exfoliated graphene layers on a SiO_2/Si substrate and of graphene nanoribbons (GNRs) grown on SiC (0 0 0 1) substrates is addressed. On the one hand, the high quality mechanically exfoliated graphene layers present a distribution of different thicknesses so it is essential to characterize the topography of the layers in the submicrometric regime. Regarding GNRs these turn out to be structures with interesting optical and electronic properties with potential applications in the field of optoelectronics and nanoelectronics. In both cases it is essential to develop fast and non-destructive approaches to determine the thickness and uniformity properties of the studied nanostructures. That is why the differential contrast technique (DRC) based on a scanning near-field optical microscope (NSOM) is implemented to achieve these resolutions, this technique consists of taking the numerical difference between the reflectivity coming from a region with substrate and a region containing graphene. In the case of monolayers we rely on the ellipsometry technique and for both systems on a multiple reflection model (graphene/ SiO_2/Si and graphene/SiC system, respectively) to know that the optical contrast can be modulated by changing the thickness of the SiO_2 or SiC layer and the incident wavelength.

With this approach, it is possible to evaluate GNRs widths with dimensions as small as 60 nm with a thickness of one or two graphene monolayers and with a spatial resolution of 40 nm. Our results demonstrate that the DRC technique is powerful for analyzing the morphology of GNRs grown on SiC (0 0 0 1) substrates as well as exfoliated monolayers of graphene on $\text{SiO}_2/$ which prove to be a promising wafer-scale platform for the development of graphene-based nanoelectronics.

In addition, the optical characterization of CdTe based materials as well as the response to evaporation of Ag thin films is shown as an approach to understand the behavior of topological insulators and the idea lies in how thin layers of metals are seen on semiconductors and their monitoring. Another group of materials as a collaboration with ETH that were studied were CuSn on polymers of different geometry and finishing processes for their synthesis. The objective is to be able to see the stress in a macro way and at the grain boundaries so *RDS* and macro *RDS* were used.

Some contributions were made with the industry, where in very general terms we will show what was done to see the potential of the techniques used in different materials and analysis interests.

Dedication

ACKNOWLEDGEMENTS

To CONACYT for the doctoral scholarship granted No. which gave me the opportunity to develop all the research shown as well as the projects that funding No.

CONTENTS

Statement of authorship	I
Abstract	II
Acknowledgements	IV
Abbreviations	VII
Packages and codes used	VIII
Symbols	IX
List of Figures	X
List of Tables	XIII
1 Introduction and Physical Background	1
1.1 Aims and Objectives	2
1.2 Thesis Outline	2
1.3 A brief history of graphene	4
1.4 Graphene structures	4
1.4.1 Graphene Monolayers and Bilayers	7
1.4.2 Graphene Nanoribbons	8
1.5 Relevant properties	9
1.5.1 Electronic properties	9
1.5.1.1 Fist approximation of numerical results	10
1.6 Importance of the optical characterization	14
2 Characterization techniques	16
2.1 Optical Spectroscopies	18
2.1.1 Ellipsometry (SE)	19
2.1.2 Near-field scanning optical microscopy (NSOM)	22
2.1.3 Diferencial Reflectance spectroscopy (RDS)	23
2.2 Atomic Force Microscopy (AFM)	24
2.2.1 Contact Mode	24
2.2.2 Tapping mode	25
2.3 Raman spectroscopy	26
2.4 Samples Description	26
3 Experimental results	28
3.1 Graphene monolayer/ SiO_2	29

3.2 Graphene nanoribbons	30
3.2.1 Sample FG163R	30
3.2.2 Sample FG166L	30
3.2.3 Sample FG166R	30
A Samples based CdTe	37
A.1 Samples Descriptions	38
A.1.1 CdTe	38
A.1.2 ZnTe	38
A.1.3 CdZnTe	39
A.2 Results an Conclusions	44
B Samples CuSn	45
B.1 Importance to study	46
B.2 Sample Descriptions	46
B.3 Results an Conclusions	47
C Industry Collaboration	54
C.1 Stratec project	55
C.2 Valeo project	58
Bibliography	59

ABBREVIATIONS

BS	Band structure
NSOM	Near-field scanning optical microscope
CCD	Charge coupled device
RAS	Reflectance anisotropy spectroscopy
GNRs	Graphene nanoribbons
SE	Spectroscopy ellipsometry
MBE	Molecular beam epitaxy
μR	Micro-Reflectance Spectroscopy
CVD	Chemical vapor deposition
R	Reflectance spectroscopy
AFM	Atomic force microscopy
BL	Buffer layer
BLG	Bilayer graphene
MLG	Monolayer graphene
DFT	Density functional theory
SEM	Scanning electron microscopy
DRC	Differential reflectance contrast
EBeam	Electron beam
RGA	Residual gas analyser
STM	Scanning tunneling microscope
1D	One-dimensional
2D	Two-dimensional
HOPG	Highly ordered pyrolytic graphite
RHEED	Reflection high-energy electron diffraction
PEM	Photoelastic modulator
RAE	Rotating-Analyzer Ellipsometry

PACKAGES AND CODES USED

Open source tools were used for the development of this thesis, both for the development of images and calculations. Everything developed in detail is hosted in the GitHub repository of the group as well as our own. It is of utmost importance to recognize that the use of these tools was fundamental for the development of the work and without their use the results of the work could not be shown.

ASE The Atomic Simulation Environment (ASE) is a set of tools and Python modules for setting up, manipulating, running, visualizing and analyzing atomistic simulations. [49]

GPAW GPAW is a density-functional theory (DFT) Python code based on the projector-augmented wave (PAW) method and the atomic simulation environment (ASE). [33]

VESTA 3D visualization program for structural models, volumetric data such as electron/nuclear densities, and crystal morphologies. [?]

PGF/TikZ PGF is a macro package for creating graphics. It is platform- and format-independent and works together with the most important TeXbackend drivers, including pdfTeXand dvips. It comes with a user-friendly syntax layer called TikZ. [?]

pst-optexp PStricks package to drawing optical experimental setups. [?]

SYMBOLS

\hbar Planck's constant (eV)

m_0 electron effective mass

(hkl) Miller indices h , k and l

E_g Energy bandgap

e electron

LIST OF FIGURES

1.1	Applications	4
1.2	Carbon allotrope timeline	5
1.3	uno-dos	6
1.4	uno-dos	6
1.5	Structure of armchair GNRs, which are the ones we study throughout this thesis, are schematized with H at the end bonds.	7
1.6	a) Band structure of graphene with the respective projections in the k_y and k_x plane, the insight shows the linear dispersion is observed, i.e. near the point K and K' (Dirac Point), b) Honeycomb lattice of graphene, showing the unit cell corresponding to two non-equivalent atoms A and B.	8
1.7	uno-dos	9
1.8	10
1.9	Structure of armchair GNRs, which are the ones we study throughout this thesis, are schematized with H at the end bonds.	11
1.10	uno-dos	12
1.11	Structure of armchair GNRs, which are the ones we study throughout this thesis, are schematized with H at the end bonds.	13
1.12	Structure of armchair GNRs, which are the ones we study throughout this thesis, are schematized with H at the end bonds.	14
2.1	Diagram showing the light-matter interaction for semiconductor nanostructures, the processes of emission, transmission, absorption and scattering can be observed. [17, 82, 95]	18
2.2	Schematic of how light is reflected in a nanostructure, where E_{ip} , E_{is} , E_{rp} and E_{rs} are the electromagnetic fields for incident and reflected light with polarization s and p respectively	19
2.3	the waves	20
2.4	It can be seen a) sample with rough surface, b) optical model that is composed of the rough surface and the bulk layers, where d_s and f are the thicknesses of the rough surface.	21
2.5	Schematic of SE coupled to a vacuum chamber used in this work, where XE is the xenon lamp, M_{1L} and M_{2L} corresponding to the first mirror array which incident the light at the entrance of the monochromator, at the output we have M_1 and M_2 then it passes through a polarizer with an angle of $\theta = 30^\circ$, hits the sample inside the chamber with an angle of $\theta = 64^\circ - 70^\circ$ and its reflection, goes to the rotating polarizer and then the signal is detected by the photomultiplier	22
2.6	Schematic of	23

2.7 Schematic of RDS coupled to a vacuum chamber used in this work, where XE is the xenon lamp, $M1_L$ and $M2_L$ corresponding to the first set of mirrors incident the light at the input of the monochromator, at the output we have $M1$ and $M2$ then it passes through a polarizer with an angle of $\theta = 45^\circ$, impinges on the sample inside the chamber with an angle of $\theta = 4.5^\circ$ and its reflection is detected by the photomultiplier.	23
2.8 Schematic of RDS coupled to a vacuum chamber used in this work, where XE is the xenon lamp, $M1_L$ and $M2_L$ corresponding to the first set of mirrors incident the light at the input of the monochromator, at the output we have $M1$ and $M2$ then it passes through a polarizer with an angle of $\theta = 45^\circ$, impinges on the sample inside the chamber with an angle of $\theta = 4.5^\circ$ and its reflection is detected by the photomultiplier.	26
3.1 Carbon allotrope timeline	29
3.2 Carbon allotrope timeline	30
3.3 Carbon allotrope timeline	31
3.4 Carbon allotrope timeline	31
3.5 Carbon allotrope timeline	32
3.6 Carbon allotrope timeline	32
3.7 Carbon allotrope timeline	33
3.8 Carbon allotrope timeline	33
3.9 Carbon allotrope timeline	34
3.10 Carbon allotrope timeline	34
3.11 Carbon allotrope timeline	35
3.12 Carbon allotrope timeline	36
A.1 all the data	39
A.2 all the data	40
A.3 all the data	41
A.4 all the data	42
A.5 Carbon allotrope timeline	43
B.1 Schematic diagram of graphene properties	47
B.2 RDS signal for the 1SLM+PP sample in different zones.	48
B.3 RDS signal for the 2SLM sample in different zones.	49
B.4 RDS signal for the 2SLM+PP sample in different zones.	50
B.5 RDS signal for the 3SLM+PP sample in different zones.	51
B.6 Schematic diagram of graphene properties	51
B.7 Schematic diagram of graphene properties	52
B.8 Schematic diagram of graphene properties	52
B.9 Schematic diagram of graphene properties	52
B.10 Schematic diagram of graphene properties	53

B.11 Schematic diagram of graphene properties	53
C.1 Micro Reflectance setup into dark configuration.	55
C.2 GUI development to analysis.	56
C.3 Image analysis of micro-device measure, at top locate the diagram of this device, where the study zone is enclosing. At center shown an image measured inside the spectral range with the marks of analyzed zones. Finally, at both sides the corresponding spectral results of each analyzed zones, in each of these denotes the depth result obtained through the fit. .	57
C.4 Three shapes of characterized samples.	58

LIST OF TABLES

2.1	Description of graphene and GNRS samples studied	26
A.1	Samples studied from the <i>CdTe</i> family	38
B.1	Description of 4 <i>CuSn</i> samples studied	46



1

INTRODUCTION AND PHYSICAL BACKGROUND

This chapter discusses the theoretical framework related to graphene and GNRs and the importance of two-dimensional materials. It is currently a very well-studied topic, so interesting properties that have real applications in the field of electronics will be discussed, as well as the remarkable advances in the synthesis of graphene and GNRs.

Contents

1.1	Aims and Objectives	2
1.2	Thesis Outline	2
1.3	A brief history of graphene	4
1.4	Graphene structures	4
1.4.1	Graphene Monolayers and Bilayers	7
1.4.2	Graphene Nanoribbons	8
1.5	Relevant properties	9
1.5.1	Electronic properties	9
1.5.1.1	Fist approximation of numerical results	10
1.6	Importance of the optical characterization	14

1.1 Aims and Objectives

Both graphene and graphene nanoribbons turn out to be quite interesting systems from their structure to the promising applications, the fact that we research terms of their optical and morphological properties opens the panorama for these to be investigated in-depth and to contribute to the implementation of new technologies based on this material.

The work carried out has the purpose of knowing both the optical and structural properties of two-dimensional and one-dimensional materials, we show the potential of optical techniques from the non-invasive point of view as well as the ability to study at the necessary scale of these systems for which we rely on various techniques such as Ellipsometry, DRC (differential reflectance contrast) based on NSOM (Near-field scanning optical microscope), RAMAN and AFM, the studies performed show i) that the DRC technique is powerful to analyze the morphology of GNRs grown on *SiC* substrates (0001) and is quite promising for the development of nanoelectronics based on graphene, as well as the characterization of low scale systems such as dichalcogenides, ii) that RDS is very useful to study *CuSn* on polymer even though it is a non-homogeneous material and it is still possible to rescue information related to stress in the structure, iii) The potential of SE and RDS to monitor the surface modification due to *Ag* evaporation on *CdTe* surfaces.

1.2 Thesis Outline

The content of this thesis includes 5 chapters and 2 appendices. The first chapter details the motivation to study graphene in the first instance and why it is important and challenging to perform studies for structural characterization, it also details the importance of systems based on *CdTe* as well as *CuSn*. The second chapter details the background knowledge and the state of the art of graphene, from a fundamental description to the behavior of phonons in these structures (graphene monolayers, bilayers, and nanoribbons), as well as it is necessary to highlight the electrical properties, the importance of the characterizations is addressed since the main challenge is the scalability of these materials for mass reproduction and implementation in applications. In chapter 3 we describe the characterization techniques used from the physical fundamentals to the description of the experimental setup for the acquisition of the information by which we describe NSOM, Raman, DRC, RDS. Within this chapter, we also describe the samples studied as part of this synthesis and finally how is the complete structure. Chapter 4 deals

with the experimental results for each sample studied in the techniques used, the thesis work dealt mostly with samples of monolayer and bilayer GNRs, here we will detail how it is possible to have the ability to discern these systems optically and the contribution of the research carried out. Finally, the last chapter reports the main results of the thesis, describes the discussion of the results obtained and the perspectives of the work performed. As appendixes, two different systems that were also studied as part A are those based on *CdTe* as an input to know the behavior of topological insulators which included working in a UHV environment as well as e-beam evaporation and a mass spectrometer. Which will be detailed in this section, as well as a set of samples based on *CuSn* which have a range of applications in the field of metallurgy and tracks for circuits, it is worth mentioning that the thesis work focused on the primary studies for future industrial uses and applications in various technological areas.

1.3 A brief history of graphene

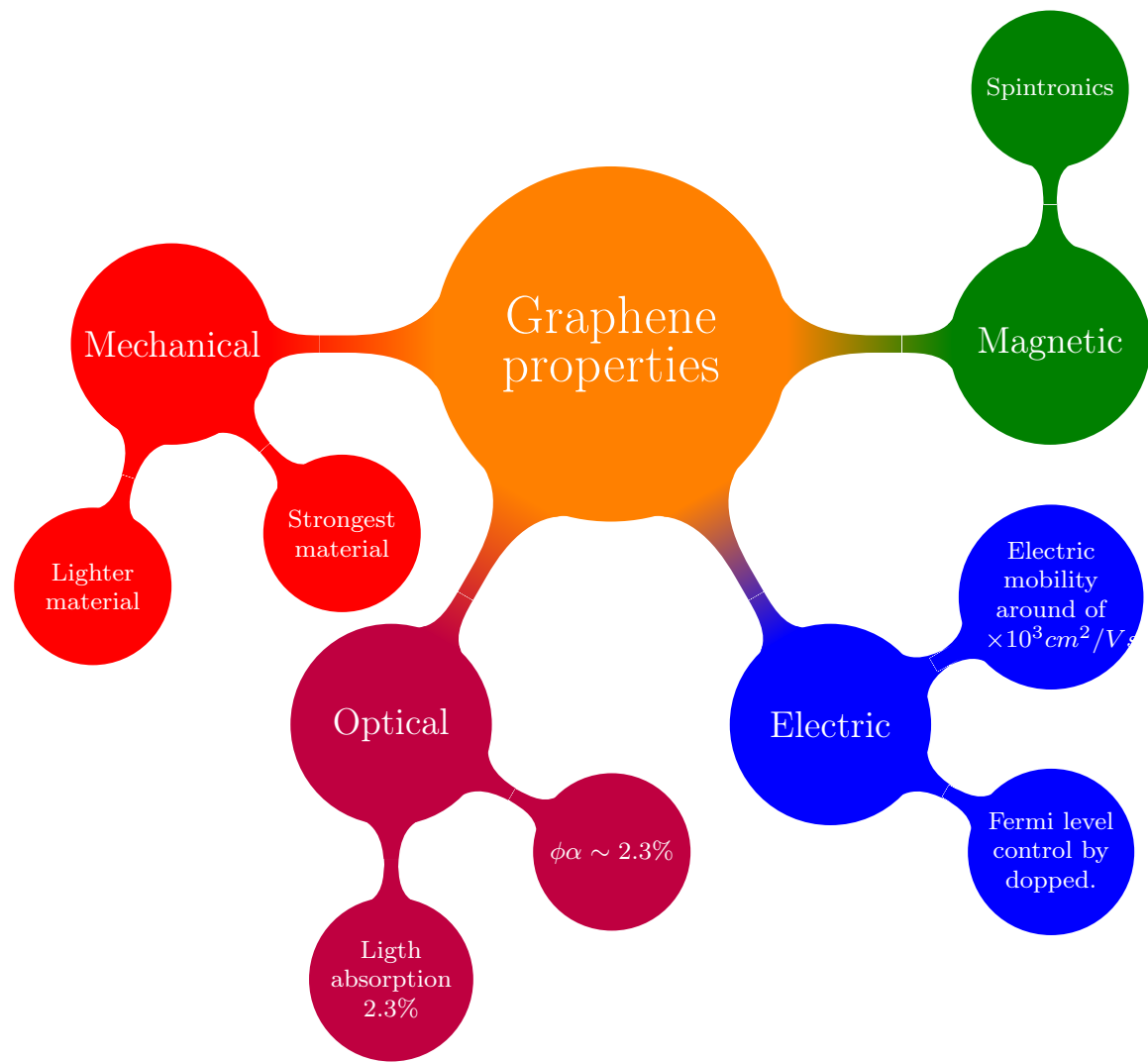


Figure 1.1: Applications

1.4 Graphene structures

Graphene is defined as a novel two-dimensional sheet of atomic thickness which is organized in a hexagonal honeycomb lattice of sp^2 -hybridized carbon atoms (a 2s orbital is mixed with two of the 2p orbitals and a total of 3 hybrid orbitals can form covalent bonds,

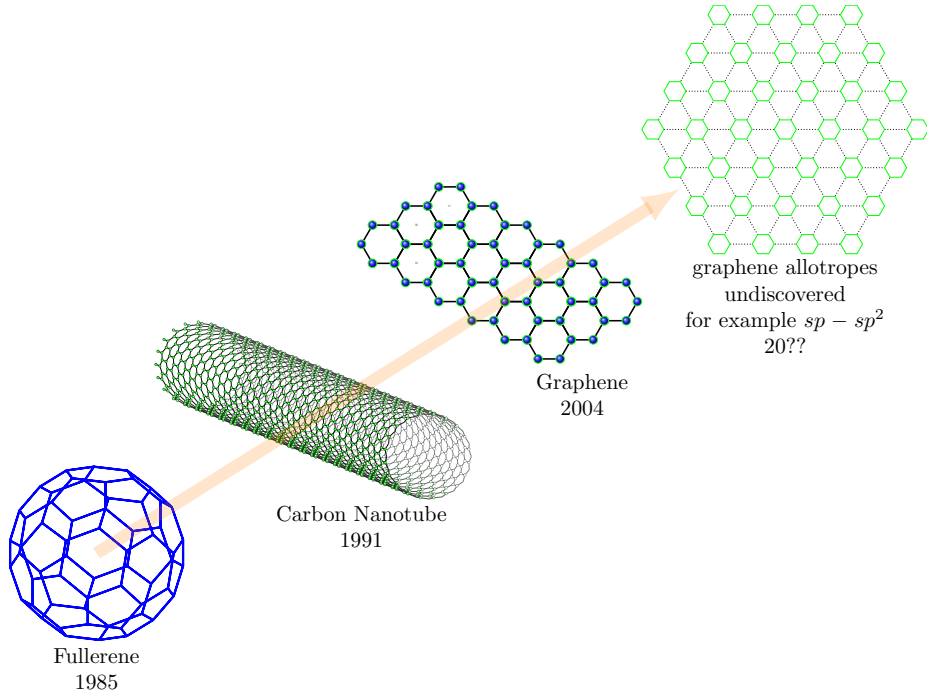


Figure 1.2: Carbon allotrope timeline

called σ bonds with neighboring carbon atoms). It has been extensively investigated since Geim and Novoselov first isolated it by performing mechanical exfoliation based on repeated peeling of highly oriented pyrolyzed graphite. For their pioneering work, which revealed the exceptional physical properties of graphene, Geim and Novoselov were awarded the 2010 Nobel Prize in Physics. Graphene has extraordinary thermal, electronic and mechanical properties, which have generated great expectations for various applications like energy storage , solar cells [81] and conversion, biosensors [80, 94], biocompatible materials [73], batteries [48], optoelectronics, electronics [19, 53, 79] and the latter is still facing challenges [65]. To date it has been extensively researched and a large number of papers have been published showing evidence of its properties and thus applications.

Given the electronic structure of graphene there are some applications that are not possible, a clear example is when you require a device you need to have an off-on process and that is why semiconductors (considerable gap) are optimal for these technological applications, however graphene has no gap and this makes it impossible to stop the flow of current so it is practically impossible to turn off at any reasonable temperature because in graphene large populations of carriers are easily produced by thermal energy and fluctuations. It is then that arises the search to induce a band gap with these graphene structures has been done much research in this area and we can mention some ways to open the gap in these structures i) applying uniaxial strain [68] ii) by dopants however this modifies the properties of graphene itself as it is a modification in the mobility of the same, iii)Graphene can grow epitaxially on SiC to form ribbons (GNRs) with widths controlled by growth conditions and post-growth annealing procedures [7, 18, 86]. The band gap of GNRs is

a function of the ribbon width and that is why controlled growth followed by reliable determination of properties such as width and thickness is of fundamental importance to tailor the properties of these nanostructures to specific applications [27].

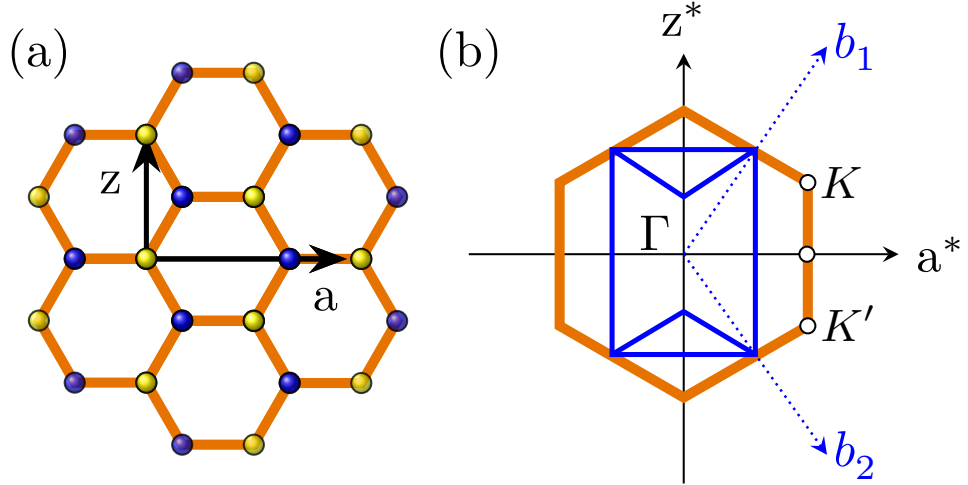


Figure 1.3: uno-dos

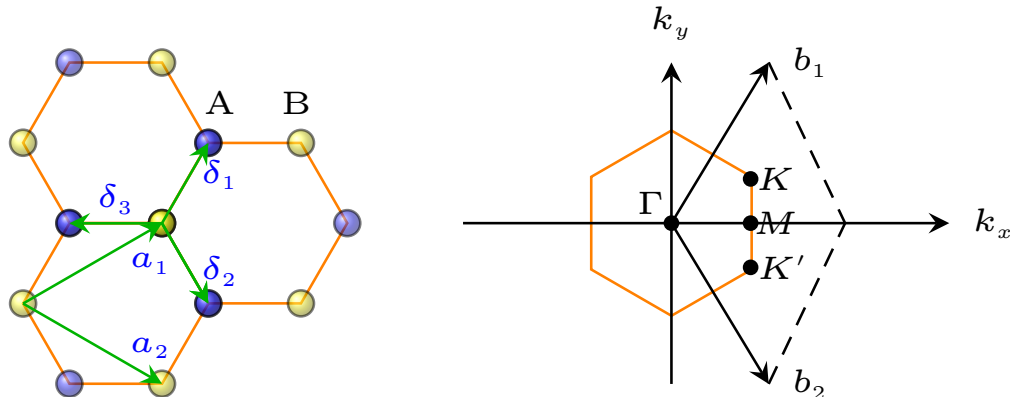


Figure 1.4: uno-dos

The structure can be seen as a triangular lattice with a base of two atoms per unit cell. The vectors are described as follows:

$$a_1 = \frac{a}{2}(3, \sqrt{3}), a_2 = \frac{a}{2}(3, -\sqrt{3}), \quad (1.1)$$

Donde $a \approx 1.42\text{\AA}$ y sus vectores de la red reciproca estan dados por

$$b_1 = \frac{2\pi}{3a}(1, \sqrt{3}), b_2 = \frac{2\pi}{3a}(1, -\sqrt{3}) \quad (1.2)$$

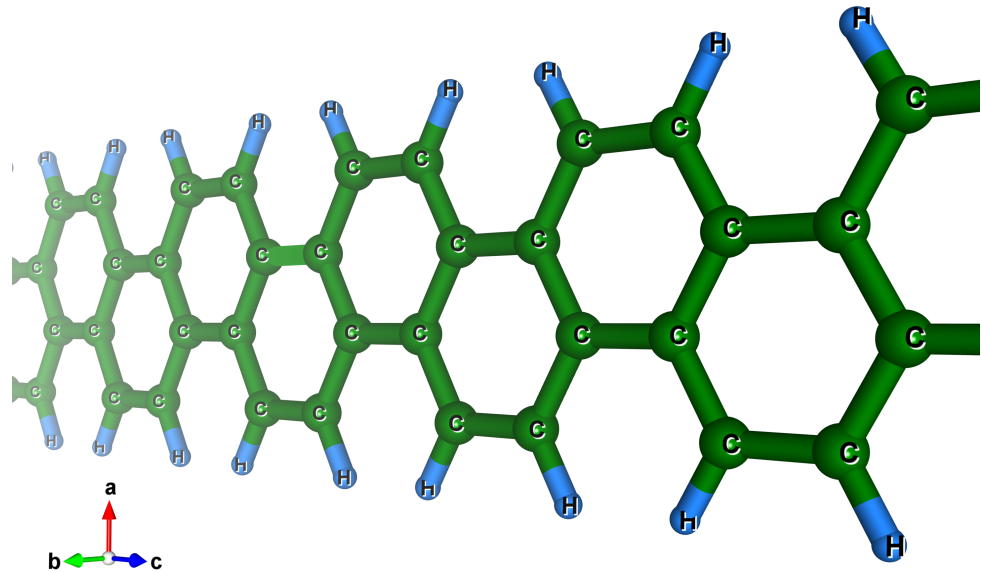


Figure 1.5: Structure of armchair GNRs, which are the ones we study throughout this thesis, are schematized with H at the end bonds.

1.4.1 Graphene Monolayers and Bilayers

The atomic structure of carbon allows it to be used in different configurations such as i) folded into fullerenes (0D), ii) rolled into nanotubes (1D), iii) stacked into graphite (3D). The carbon atoms of graphene are separated by an interatomic distance of $a = 1.42\text{\AA}$ and the primitive cell of graphene is composed of two non-equivalent atoms. As for its electronic configuration it is very important to mention that the planar orbitals form the energetically stable and localized σ bonds with the three nearest carbon atoms in the honeycomb lattice, and are responsible for most of the binding energy and elastic properties of the graphene layer so that the remaining $2p_z$ orbitals have π symmetry and the overlap of these orbital states between neighboring atoms plays an important role in the electronic properties of graphene.

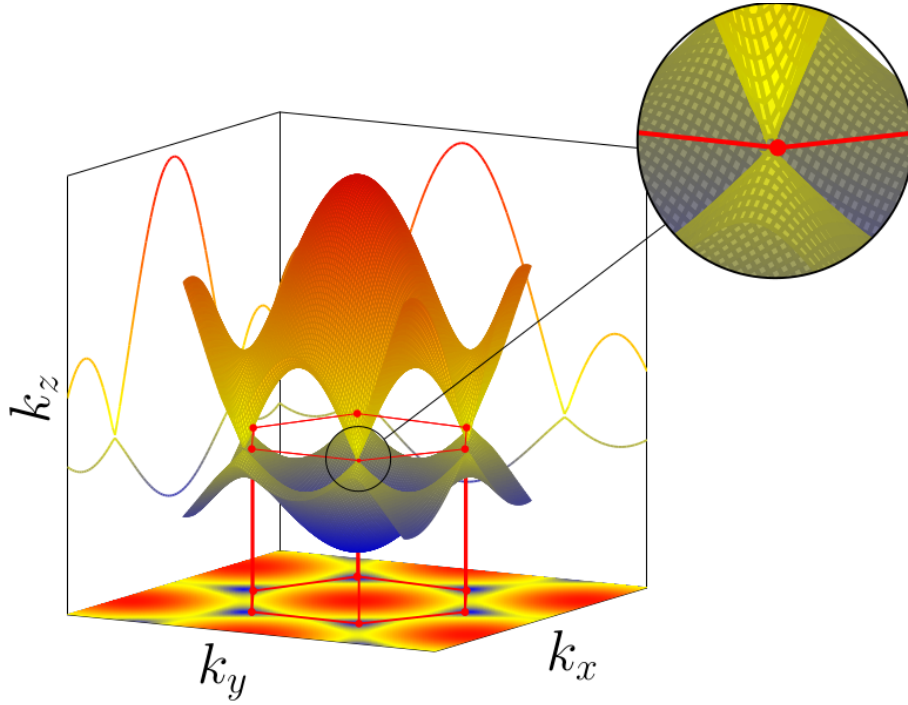


Figure 1.6: a) Band structure of graphene with the respective projections in the k_y and k_x plane, the insight shows the linear dispersion is observed, i.e. near the point K and K' (Dirac Point), b) Honeycomb lattice of graphene, showing the unit cell corresponding to two non-equivalent atoms A and B.

1.4.2 Graphene Nanoribbons

In the case of GNRs it is worth mentioning that many of their essential properties have been conducted by the tight-binding model [66, 83] and the first-principles method [85]. In the former model GNRs in armchair configuration are predicted to be metals and in the latter they are semiconductors for $N_A = 3I + 2$ where N_A is the number of dimer lines along the transverse direction corresponding to the electronic states of monolayer graphene in the presence of open boundary conditions. The energy gaps are predicted to be inversely proportional to the width of the nano-ribbons, clearly indicating the quantum confinement effect. In addition, the electronic properties are sensitive to the change in the structure of the edges recalling that there are two configurations i) armchair which are the already described in this work and ii) and zigzag [55]

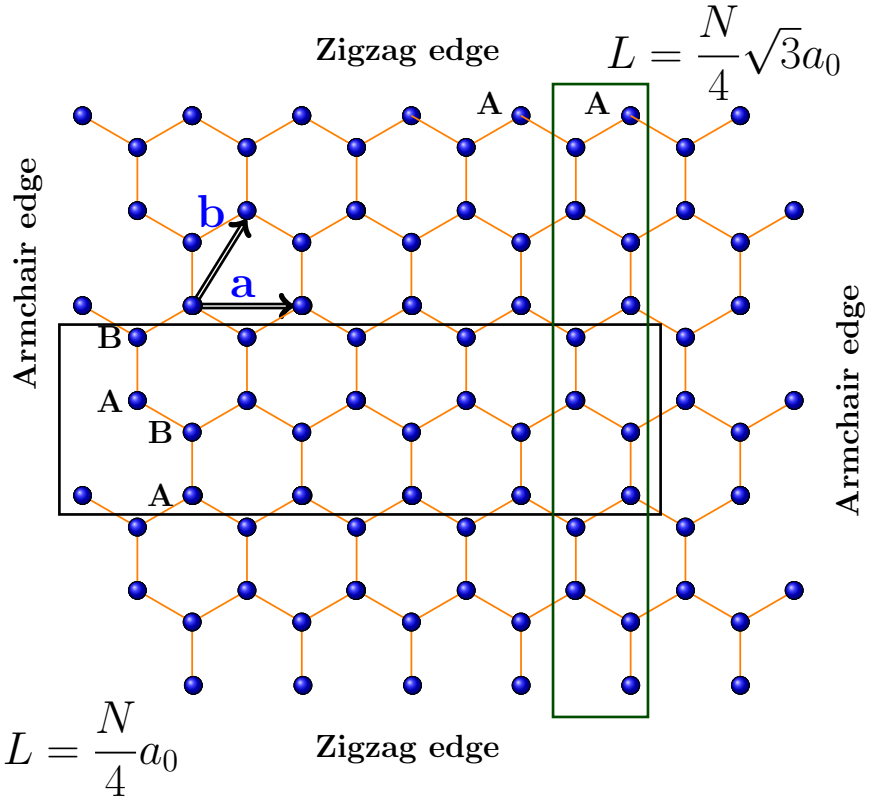


Figure 1.7: uno-dos

1.5

Relevant properties

1.5.1 Electronic properties

Graphene is being called as a material of century, although recently two-dimensional materials are the trendy, therefore the interest of graphene was decreased. But, Jarillo-Herrero *et al.* [13, 15, 16], they came to get a new hope to Graphene, this due exhibits an unconventional superconductivity under specific structure arrangement. This behavior and others important them, are exhibits by Graphene and the all gamut of structures derivative of it. Inside that gamut of Graphene structures, the GNR's are very studied by the amazing confinement that these it presents and the interesting applies as spintronic devices [46, 85]. On going on the physical background involved on it, the geometry of these structures plays the most significant role, due to the BS specifically the band gap depends on geometry of these. This means, the ribbon's dimensions affect the band gap value,

therefore the properties that can being exhibits depends on that [84]. In order to illustrate, we worked on first-principle calculations trough preset models without intention of deepens and discuss them, since this work has the aim of show experimental results obtained in this and another structures. But, it is important to break the paradigm that the experimental physicist does not can implement masterly tools created by the theorist.

1.5.1.1 Fist approximation of numerical results

The importance of employed theoretical and numerical models to improve and enhanced the understanding of results in solid and condensed matter physics was evolved by technics as Density Functional Theory. As an increasing computational capacity, it is enabled to employ more sophisticated numerical approximations taken DFT as basis. This impact in the experimental area, because provides a guide to carried out experiments and structure design [97] with possibility to get new properties. By this reason, in this works we consider this technics already implemented in powerful open codes and by simplicity and usefully environment, we use ASE interface [49]. Since ASE provides the most useful open tools in atomistic simulations, being that their python programming supply and reduce the extensive work. It is important to remark that the fundamental theory discussion will not be addressed in here, we focus on the models and technics as experimental tools therefore we discuss the results getting it. Due to the little computational resource, we purpose two GNRs structures computes trough GPAW code [26, 63], GPAW is a density-functional theory (DFT) Python code based on the projector-augmented wave (PAW) [11, 76]. Taking

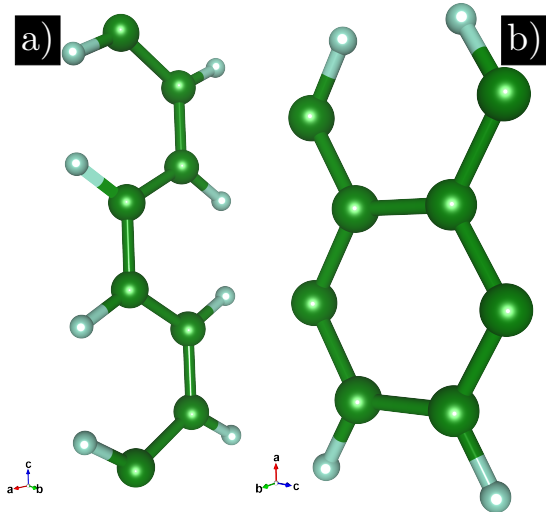


Figure 1.8

advantage of ASE environment provides some nanostructures, we take the nanoribbons function, and we adapt in according to our computational resources. Figure 1.8 shown both zigzag and armchair structures consider in our DFT calculations. With the codes employs

in our experimental research these the work are becomes friendly, then is easy to get band structure information. The given results are characteristic by these structures, because as well known the edge plays an importantly role of confinement and the consequently properties of GNRs. This approximate results expose the variety of Graphene zoo results, the simplicity of symmetry around of edge modify also properties and characteristics. The importance of calculate the BS

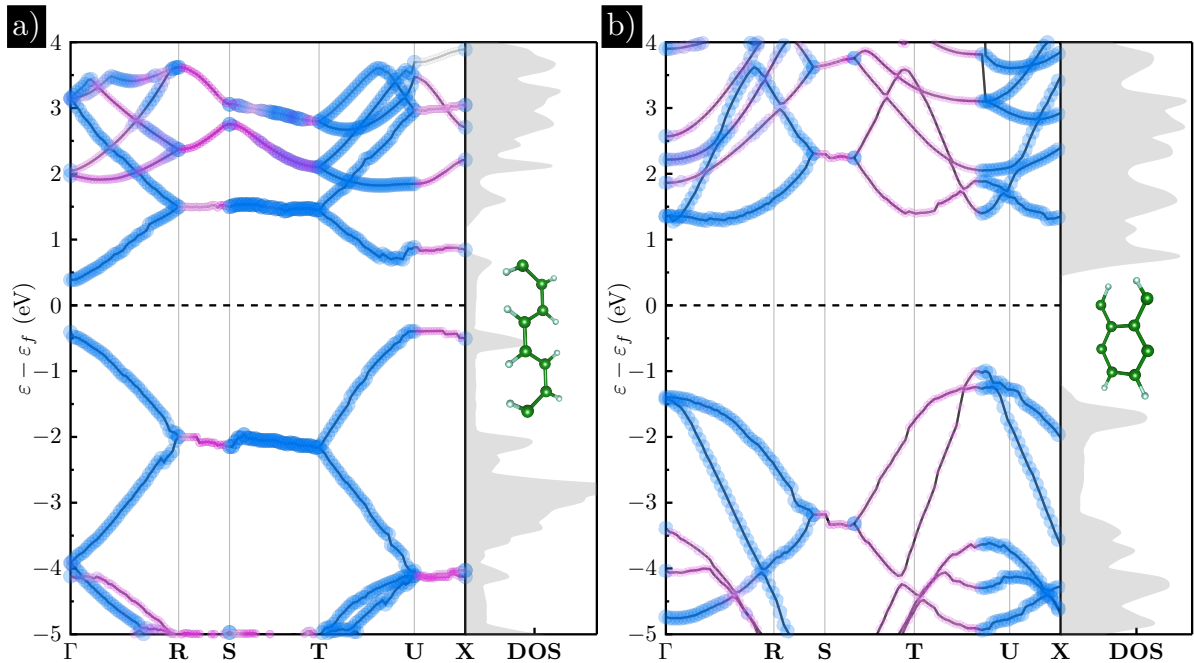


Figure 1.9: Structure of armchair GNRs, which are the ones we study throughout this thesis, are schematized with H at the end bonds.

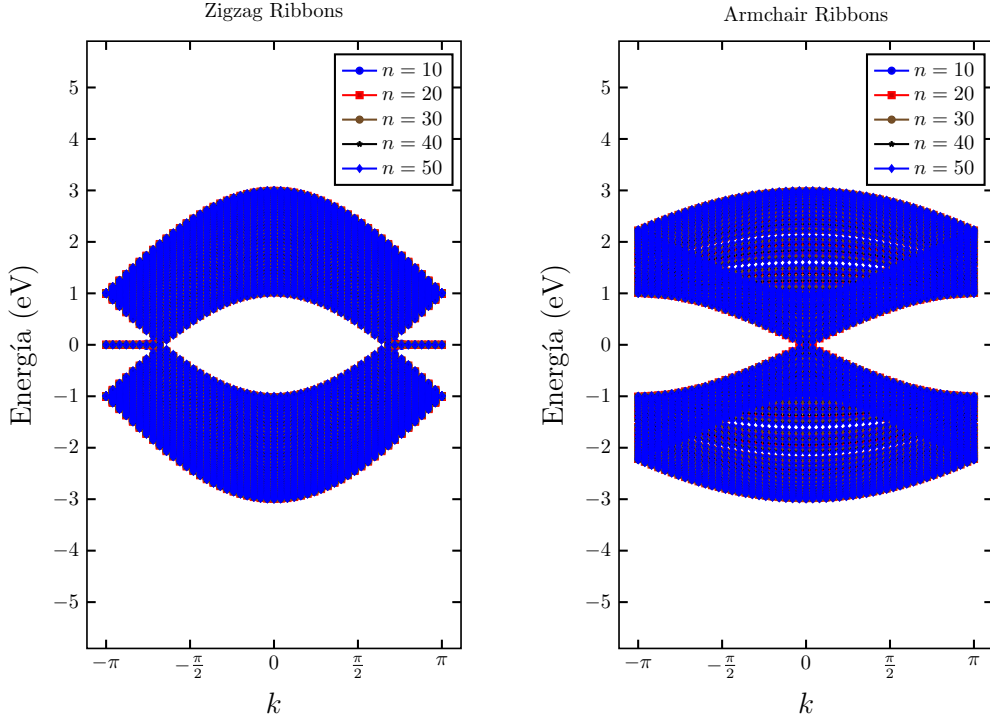


Figure 1.10: uno-dos

The objective in this section of the thesis is to use these existing computational tools to corroborate with the experimental results. theoretical and numerical models to improve and enhanced the understanding of results in solid and condensed matter physics was evolved by technics as Density Functional Theory. As an increasing computational capacity, it is enabled to employ more sophisticated numerical approximations taken DFT as basis. This impact in the experimental area, because provides a guide to carried out experiments and structure design [97] with possibility to get new properties. By this reason, in this works we consider this technics already implemented in powerful open codes and by simplicity and usefully environment, we use ASE interface [49]. Since ASE provides the most useful open tools in atomistic simulations, being that their python programming supply and reduce the extensive work. It is important to remark that the fundamental theory discussion will not be addressed in here, we focus on the models and technics as experimental tools therefore we discuss the results getting it. Due to the little computational resource, we purpose two GNRs structures computes trough GPAW code [26, 63], GPAW is a density-functional theory (DFT) Python code based on the projector-augmented wave (PAW) [11, 76].

Taking advantage of ASE environment provides some nanostructures, we take the nanoribbons function, and we adapt in according to our computational resources. Figure 1.8 shown both zigzag and armchair structures consider in our DFT calculations. With the codes employs in our experimental research these the work are becomes friendly, then is easy to get band structure information. The given results are characteristic by these structures, because as well known the edge plays an importantly role of confinement and the consequently properties of GNRs. This approximate results expose the variety of

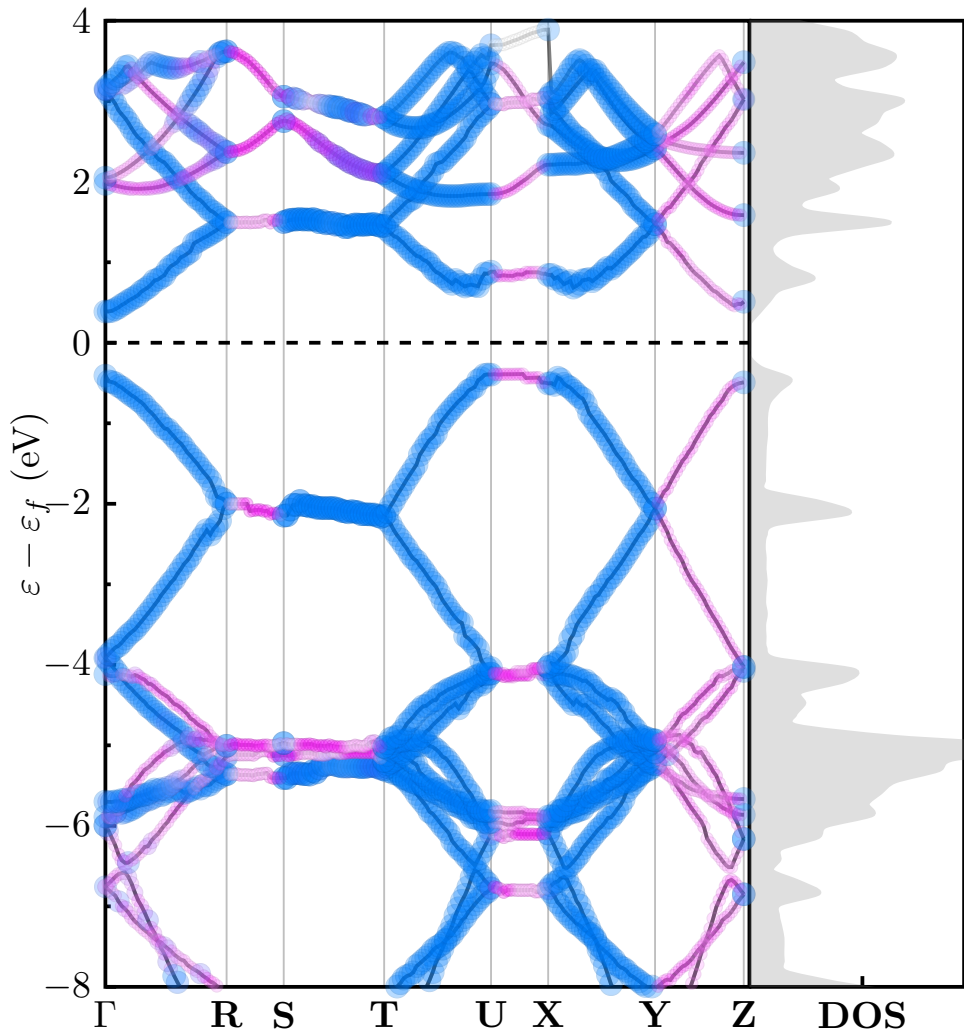


Figure 1.11: Structure of armchair GNRs, which are the ones we study throughout this thesis, are schematized with H at the end bonds.

Graphene zoo results, the simplicity of symmetry around of edge modify also properties and characteristics. The importance of calculate the BS

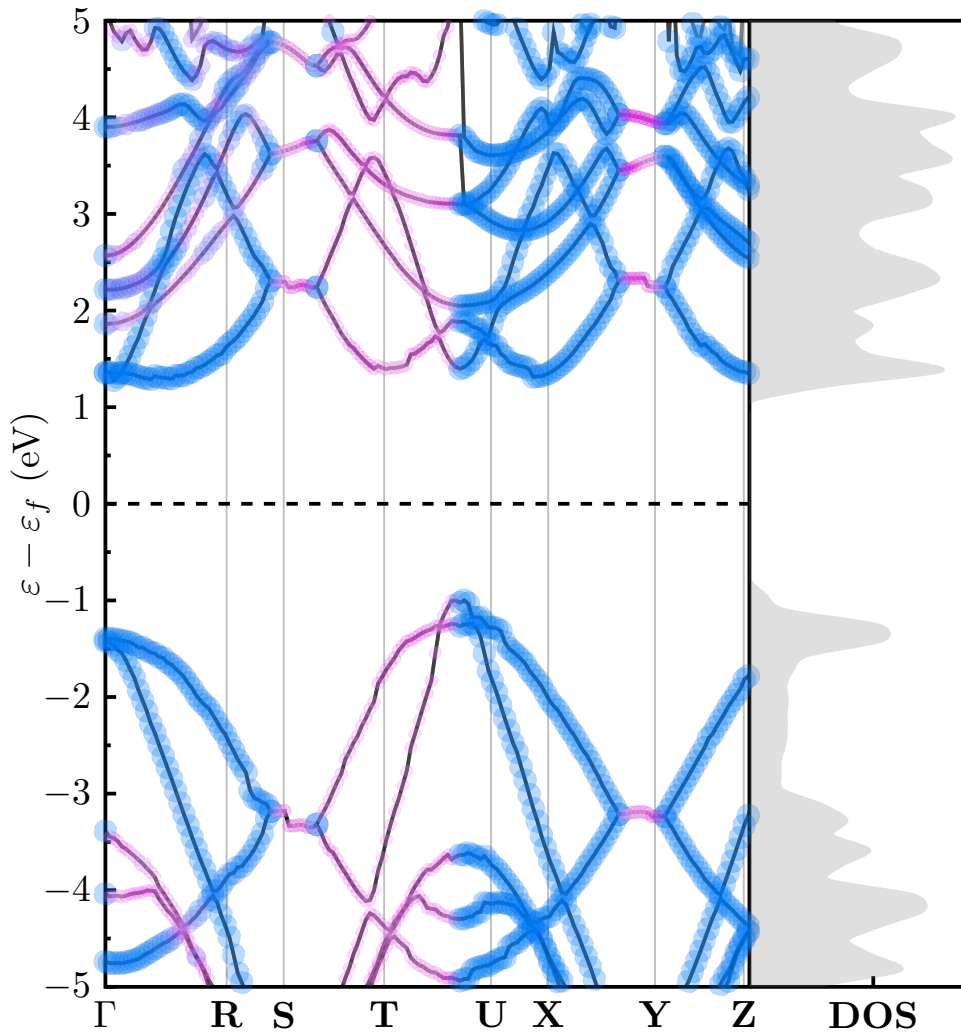


Figure 1.12: Structure of armchair GNRs, which are the ones we study throughout this thesis, are schematized with H at the end bonds.

1.6

Importance of the optical characterization

In addition to the interest of graphene layers (from 1 layer up to 10), graphene nanostructures such as the ones we have studied which are GNRs show a wide interest for various potential electronic applications. It has been studied that nanostructures can offer a direct band gap due to quantum confinement of charge carriers and that it depends on both lateral width and termination which is required for switching devices and even for DNA sequencing tools.



CHARACTERIZATION TECHNIQUES

In this chapter, we will address the characterization techniques used because they provide us information of the material under study, as a brief description, we start with SE which allows us to know the fingerprint of our material and through the construction of models to know optical constants, film structure (thickness) among others. Raman spectroscopy is a non-destructive technique that allows us to know the vibrational modes of the molecules so we can know information about the chemical structure and even crystallinity of the material. RAS or RDS is a surface-sensitive optical modulation technique that allows us to know information about surface anisotropies and the interactions with the multiple layers of a heterostructure, we will also approach DRC which is based on NSOM coupled with AFM to visualize and analyze at this resolution morphology and reflectivity of various materials simultaneously. The central part of this work deals with graphene samples will be described including their synthesis, which were performed by CNR/NANOTEC in Italy and the Paul Drude Institute in Germany. In the case of CuSn samples they were synthesized at the Swiss Federal Institute of Technology in Zurich (ETH).

Contents

2.1 Optical Spectroscopies	18
2.1.1 Ellipsometry (SE)	19
2.1.2 Near-field scanning optical microscopy (NSOM)	22
2.1.3 Diferencial Reflectance spectroscopy (RDS)	23
2.2 Atomic Force Microscopy (AFM)	24
2.2.1 Contact Mode	24
2.2.2 Tapping mode	25
2.3 Raman spectroscopy	26
2.4 Samples Description	26

2.1 Optical Spectroscopies

To begin the following section it is necessary to describe what we mean when we talk about optical spectroscopy and we refer to the study of the interaction of light with the material where three parameters influence: i) intensity, ii) wavelength and iii) polarization state, whereby the processes of absorption, emission and scattering are studied. [42]. As in Fig.2.1

In this work we address techniques that allowed us to provide information on the reflectivity, morphology and absorption obtained from different structures such as those based on graphene, CdTe and CuSb, in particular we focused on graphene monolayers and nanoribbons, which was a challenge because it must consider the dimensions of the layers and the contrast obtained from the different zones

As mentioned in the theory section, there is a need to analyze with non-invasive techniques the morphology of different graphene layers, there are several powerful and interesting alternatives such as RAMAN, however they have the limitation that the analysis spot is larger in diameter than what is covered by a layer of graphene and actually covers an area of multiple thicknesses, so it can not be known specifically or spatially in small areas. Since one of the most common ways to obtain graphene is by exfoliating it, in this specific case the way proposed throughout this thesis is to use the NSOM based contrast technique which will allow us to know the reflectivity of zones at an adequate scale as a fundamental technique. The supporting techniques used were ellipsometry, RDS, and AFM, which are described below.

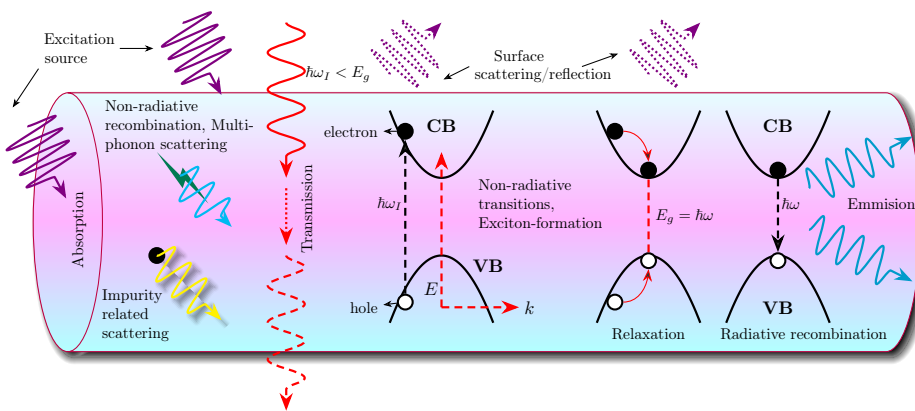


Figure 2.1: Diagram showing the light-matter interaction for semiconductor nanostructures, the processes of emission, transmission, absorption and scattering can be observed. [17, 82, 95]

2.1.1 Ellipsometry (SE)

Ellipsometry is an optical technique used for the characterization and observation of events in both an interface and a film, i.e. it takes advantage of the reflection or transmission of incident light from various materials that we wish to study. It is responsible for measuring the change of polarized light when reflecting or transmitting light in a sample and is called ellipsometry because the polarized incident light changes its polarization to elliptical after reflecting or transmitting in the sample. It is widely used for its non-perturbing character [3] (when the wavelength and intensity of the light beam are properly chosen) and in this sense, it can be measured in-situ and ex-situ, SE is highly sensitive to interfacial defects such as oxidation, evaporation of thin films among others [28].

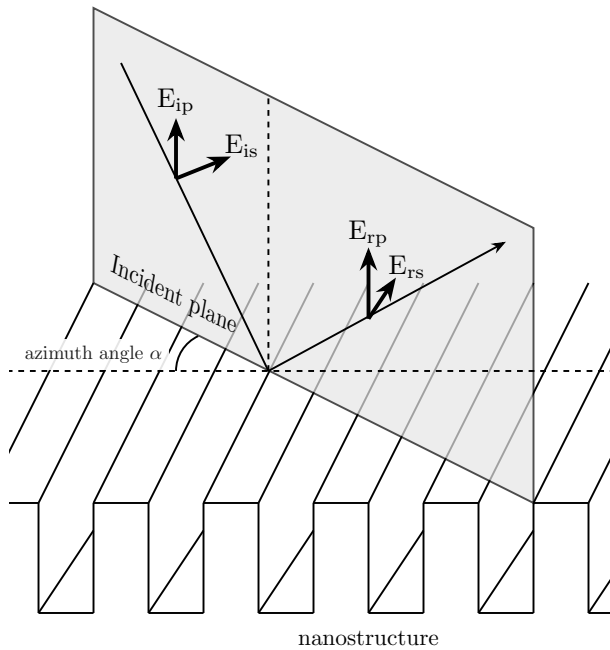


Figure 2.2: Schematic of how light is reflected in a nanostructure, where E_{ip} , E_{is} , E_{rp} and E_{rs} are the electromagnetic fields for incident and reflected light with polarization s and p respectively

The interaction of the electric fields in a nanostructure and the distribution of the polarizations can be seen in Fig. 2.2. SE allows us to measure two fundamental values (ψ , Δ) where ψ represents the amplitude ratio and Δ refers to the phase difference between p and s polarization, this is done in a wavelength range in our case from 210nm to 650nm however, it can be done in the infrared range depending on the material under study and the properties of interest.

The reason for using SE in the developed work is to know the dielectric function of graphene, GNRs and CdTe-based materials as we can acquire information about the band

structure and optical transitions [28, 92].

To understand this change of polarization when reflecting off the sample we can look at Fig. 2.3 where linearly polarized light is described as an electromagnetic wave with orthogonal electric \mathbf{E} and magnetic \mathbf{B} fields which are characteristic of light since it is a periodic transverse electromagnetic disturbance [57]. Linear polarization refers to the existence of an electric field orientation when the wave propagates in the z direction, but the \mathbf{E} field (and the \mathbf{B} field) oscillates in x (and the \mathbf{B} field in y), hence the transverse nature of light waves. Circularly polarized light tells us that as the wave propagates the vector \mathbf{E} rotates with the end point of the vector \mathbf{E} tracing a circle, and for our case where the light is elliptically polarized hence an ellipse is shown as the projected locus of the end points of \mathbf{E} as the wave propagates, but \mathbf{E} also changes in magnitude and hence traces an ellipse.

Therefore the polarization state is defined as follows:

$$\tan(\Psi)\varepsilon^i\Delta = a \quad (2.1)$$

Where r_s is the complex amplitude reflectance for the s-polarization, r_p is the complex amplitude reflectance for the p-polarization, and Ψ is the ellipsometric magnitude reflectivity ratio, and Δ is the ellipsometric phase term [80].

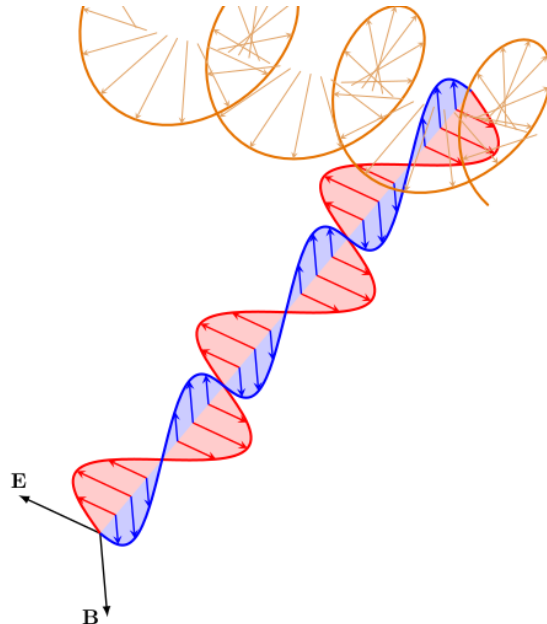
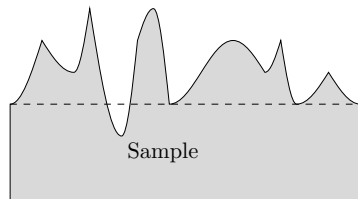


Figure 2.3: the waves

In order to obtain the experimental parameters we performed our experiments in a wavelength range from 210nm to 650nm (1.9ev to 5.9ev) in general, however we focus on

the wavelength of our interest depending on the material under study. So spectroscopic ellipsometry is able to provide unique responses for material parameters (See Fig 2.4) in addition to having a high sensitivity to material properties, it is worth mentioning that we can obtain both the real and imaginary part of the dielectric function without the need to perform KK analysis.

(a) Sample structure



(b) Optical model

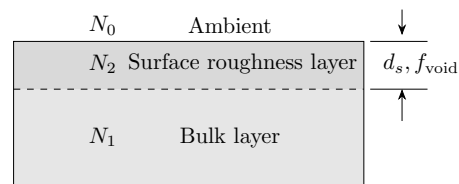


Figure 2.4: It can be seen a) sample with rough surface, b) optical model that is composed of the rough surface and the bulk layers, where d_s and f are the thicknesses of the rough surface.

The photometric ellipsometer implemented at IICO (Instituto de Investigacion en Comunicacion Optica) has the RAE configuration which takes advantage of the modulation of the signal obtained thanks to a rotating analyzer, the array (see Fig. 2.5) starts with a 75 W Xenon light source (Hammamatsu Photonics) and then passes through an array of mirrors (with focal length $f/6$) that lead to the monochromator (Jobin-Yvon-Spex with two diffraction gratings of 1200 lines/mm and 600 lines/mm) just in order to make the scan with monochromatic light, then the collimated light thanks to a pair of mirrors (with focal length $f/10$) is directed through a linear polarizer (Rochon of *Optics for Research*) which is at an azimuthal angle 30° with respect to the angle of incidence and we focus it on the sample which is at an oblique angle of 70° , the reflection passes again through a linear analyzer (inverted polarizer) which is rotating at a fixed angular frequency of 856Hz, then this response is collected with a photomultiplier to measure the DC component we use a Keithley Multimeter 2000 multimeter and the AC signal is measured with a Lock-In amplifier Stanford Research System model SRS350.

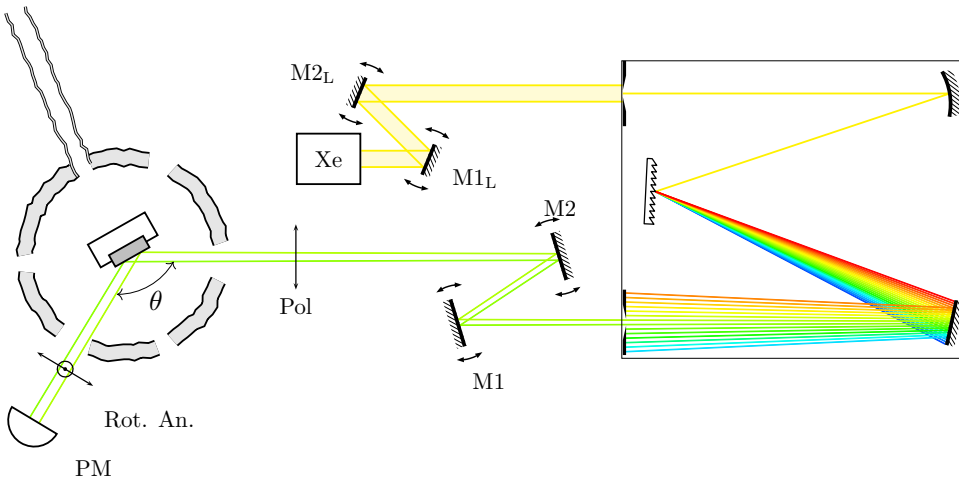


Figure 2.5: Schematic of SE coupled to a vacuum chamber used in this work, where Xe is the xenon lamp, $M1_L$ and $M2_L$ corresponding to the first mirror array which incident the light at the entrance of the monochromator, at the output we have $M1$ and $M2$ then it passes through a polarizer with an angle of $\theta = 30^\circ$, hits the sample inside the chamber with an angle of $\theta = 64^\circ - 70^\circ$ and its reflection, goes to the rotating polarizer and then the signal is detected by the photomultiplier

The acquired signals from both the multimeter and lock-in signals are processed with routines developed in Python so that the pseudo-dielectric function, absorption and layer thicknesses can be visualized.

2.1.2 Near-field scanning optical microscopy (NSOM)

Some of these SPM modes were SNOM (Scanning Nearfield Optical Microscopy), but there are at least 20 different modes of AFM. SNOM is an example of using the close contact and position control of the AFM to measure properties of the surface other than topography (in this case, optical properties)

By combining optical spectroscopy with scanning near-field optical microscopy (SNOM)

The Nanonics commercial system available at the IICO, mostrada , which was fundamental for the development of this work, has the capacity to make a scan to know the amount of reflected light and simultaneously know the morphology of the surface, that is to say, in a coupled AFM-NSOM way. We call the magnitude of the scans "windows" and they were studied from small areas $2\mu m \times 2\mu m$ to $25\mu m \times 25\mu m$

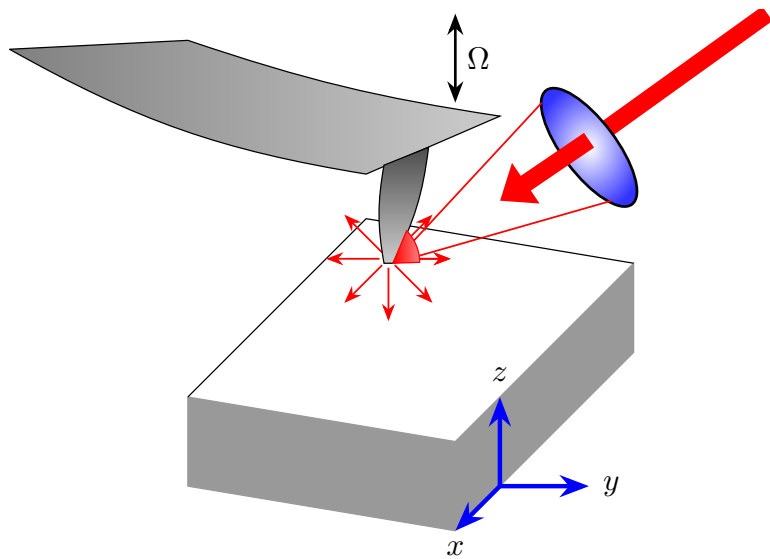


Figure 2.6: Schematic of

2.1.3 Differential Reflectance spectroscopy (RDS)

In the case of modulated spectroscopies these have been recognized to investigate optical properties that allow us to know the electronic structure of the material and therefore a variety of physical parameters.

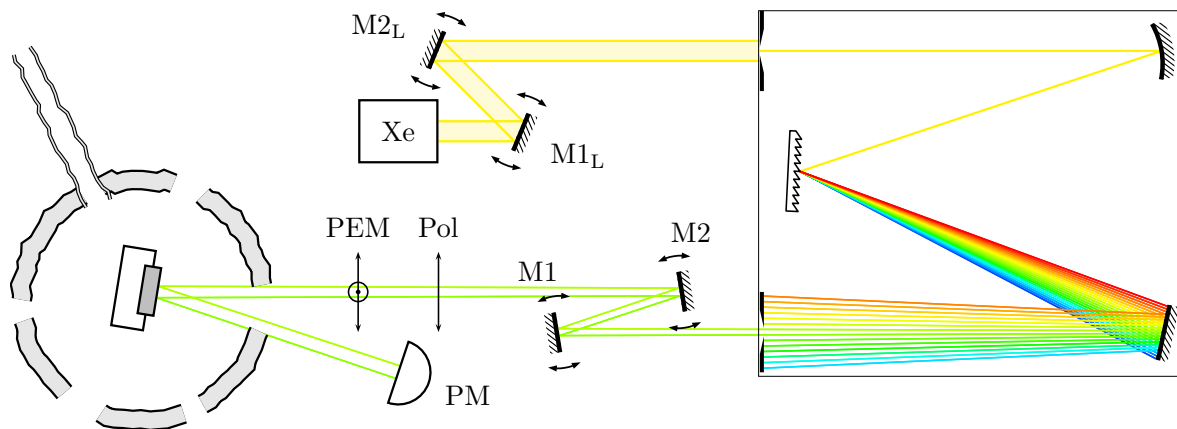


Figure 2.7: Schematic of RDS coupled to a vacuum chamber used in this work, where XE is the xenon lamp, $M1_L$ and $M2_L$ corresponding to the first set of mirrors incident the light at the input of the monochromator, at the output we have $M1$ and $M2$ then it passes through a polarizer with an angle of $\theta = 45^\circ$, impinges on the sample inside the chamber with an angle of $\theta = 4.5^\circ$ and its reflection is detected by the photomultiplier.

2.2

Atomic Force Microscopy (AFM)

To get into context about atomic force microscopy (AFM) [9, 10] we must first describe the STM technique is based on studying the phenomenon of electron tunneling in conductive surfaces its inventors were *G. Binning* and *H. Rohrer* for which were awarded the Nobel Prize in Physics in 1986 and for such an interesting invention now have been investigated several metals and semiconductors [23, 32, 101] at the atomic scale which has allowed a series of advances in progress, a disadvantage that has the STM is that there needs to be electrical conduction in the samples (it's possible to obtain images of metals and conductive samples even HOPG but not in ambient conditions but in ultra-high vacuum environments [69]) because the tunnel current flows between the tip and the sample, Even so, it was realized that if the distance between tip and the sample is very small the current can flow, and collateral forces are appreciated, this is where the search of *Binning* comes in to apply it to insulating surfaces, so the AFM is developed, which is based on the repulsion force between tip and surface and no longer has the limitation of STM [10].

AFM was developed to start the principle of a measuring device, not only the forces arising from inter-atomic interactions, but also other forces such as those due to electric and magnetic fields [9].

The principle of AFM in terms of surface "sensing" consists of a sharp tip on a cantilever (See Fig. 1) to scan a specific area and due to the short range attractive forces between the surface and the tip causing it to flex to the surface as the approach increases, the repulsive forces also induce the tip to flex, the way in which these changes in tip deflection are detected in general is by incident a laser on the cantilever and the changes in the direction of the reflected beam translate into changes in the morphology of the sample under study.

There are some ways in which morphology can be studied in AFM, in this case we will describe the contact mode and the tapping mode, this last way was the one used for the characterizations.

2.2.1 Contact Mode

This mode can be considered standard and is a very powerful and used technique that consists of the tip being in contact with the surface and by repulsive force, the tip is deflected so that the respective topography is obtained, it is fast since

it is not necessary to add the oscillation measurements and thus avoid time to obtain the image.

However, there are some points to consider that in this mode i) given the repulsion between sample and tip, the sample can be damaged in the scan or the tip by abrupt changes in the scanning surface ii) because tip and sample are in constant contact in addition to the normal force applied between them, lateral forces are experienced [1, 23, 25]

2.2.2 Tapping mode

The tapping mode consists in that the cantilever vibrates at a resonance frequency in such a way that when approaching the sample, the tip slightly touches the surface in the final part of each oscillation, this is represented in a decrease of the amplitude and then with feedback cycle maintains this decrease in a preset value and the sweep is performed and in this way the topographic image of the surface is obtained, something that distinguishes it is that lateral forces are practically eliminated and the sample under study is not damaged [22, 75].

2.3 Raman spectroscopy

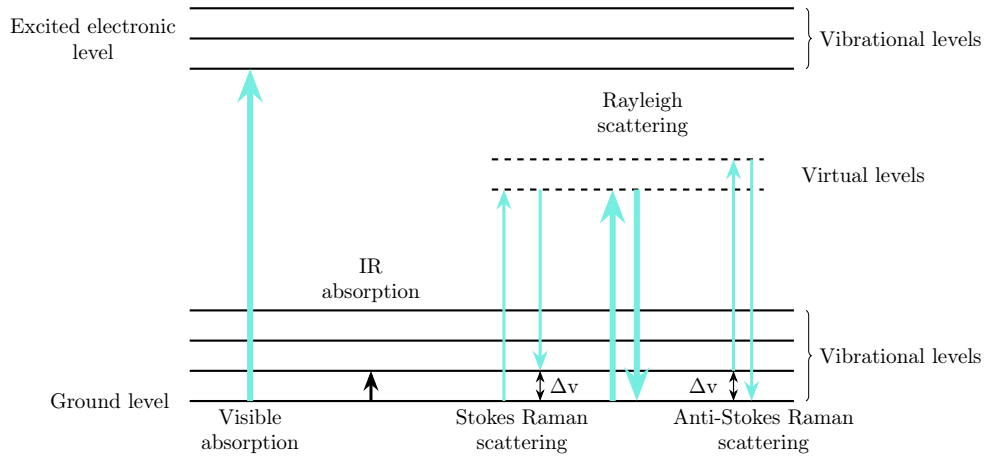


Figure 2.8: Schematic of RDS coupled to a vacuum chamber used in this work, where XE is the xenon lamp, M_{1L} and M_{2L} corresponding to the first set of mirrors incident the light at the input of the monochromator, at the output we have M_1 and M_2 then it passes through a polarizer with an angle of $\theta = 45^\circ$, impinges on the sample inside the chamber with an angle of $\theta = 4.5^\circ$ and its reflection is detected by the photomultiplier.

2.4 Samples Description

The studied samples described in the following table were synthesized at the Paul Drude Institute in Berlin, Germany by the group led by Dr. Marcelo Lopes.

	Description	Average width
FG163L	QFS BL-GNRs on SI SiC(0 0 0 1)	240nm
FG166L	QFS BL-GNRs on SI SiC(0 0 0 1)	120nm
FG166R	QFS BL-GNRs on SI SiC(0 0 0 1)	150nm
FG271	ML-GNRs on buffer layer/SiC(0 0 0 1)	
FG944	QFS-BL-G on n-type SiC(0 0 0 1)	

Table 2.1: Description of graphene and GNRS samples studied

The development of non-invasive optical techniques for the study of various materials

brings with it endless applications in the case of graphene in the field of electrinocs and microelectronics,

y efectivamente se observa un cambio muy notorio en la respuesta de RDS en primera instancia esta se trato de emularla con un modelo de strain en la zona de alrededor 4ev, el s

El proceso para s

- Limpieza de la muestra con tricloroetileno, enseguida enjuagar con
-

Las transiciones localizadas en 2.5ev y 4ev muestran un cambio incluso la forma de linea tiene una evolucion maximizando estas donde se observa por una parte que se tiene un deposito de Ag e incluso se puede modelar con la funcion dielectrica que se obtiene antes y despues de los depositos, tal como comenta el diagrama en la parte tecnica de la misma se puede obtener diversas propiedades con esta forma de linea tanto del espesor de las peliculas como espesor de los oxidos que se crecen sobre la muestra

En el caso de las muestras de grafeno, descritas como los nanolistones se puede observar que podemos tanto obtener informacion de las capas de las cuales estan compuestas como de la resolucion lateral d ela misma. La resolucion que nos brinda NSOM nos permite tanto obtener informacion estructural como optica, al estar haciendo incidir sobre la punta de NSOM e ir barriendo, la comparacion o el tranlape que se puede hacer es bastante util por que nos damos cuenta que realizando un modelo de tres capas de la reflectividad donde se involucran los coeficientes de reflexion de fresnel los cuales se explican en la parte teorica de la misma podemos entender como un sistema de silicio, oxido de silicio, multiples capas de de grafeno y aire, siempre los medios superiores e inferior los consideramos como infinitos con el fin de mantener aislado en sistema y que nos pueda brindar una mejor respuesta y mas cercana a la real que vemos de manera experimental, en el caso de las muestras exfoliadas y en el caso de los nanolistones de grafeno tenemos carburo de silicio en su forma hexagonal para de esta forma sintetizar el grafeno ya que su configuracion cristalina es hexagonal, la manera en la que se sintetiza y fue descrita en la parte de muestra se puede apreciar que la terminacion en los bordes del edge de los escalones se suelen acumular demasiado que nos brinda incluso en muchos casos multiples monocapas de grafeno, tal como se menciona en una manera comun del crecimiento, sin embargo con todas las condiciones esperadas podemos tener un crecimiento controlado.

3

EXPERIMENTAL RESULTS

In this section we will detail the results in first instance of a series of samples i) Graphene exfoliated on SiO_2 . ii) GNRs of different thickness and width, in particular we focus on studying them by the DRC technique, however we rely on the previous techniques as it is convenient to rescue information for their complete characterization.

Contents

3.1	Graphene monolayer/SiO_2	29
3.2	Graphene nanoribbons	30
3.2.1	Sample FG163R	30
3.2.2	Sample FG166L	30
3.2.3	Sample FG166R	30

3.1 Graphene monolayer/ SiO_2

Como se menciono el apartado de physical background la caracterizacion de grafeno resulta de bastante interes tanto tecnologico como cientifico, por lo que surge la necesidad de desarrollar, implementar, mejorar o modificar tecnicas opticas no invasivas que nos permitan caracterizar grafeno, una de las formas en las que se puede obtener es mediante exfoliacion mecanica la cual radica en

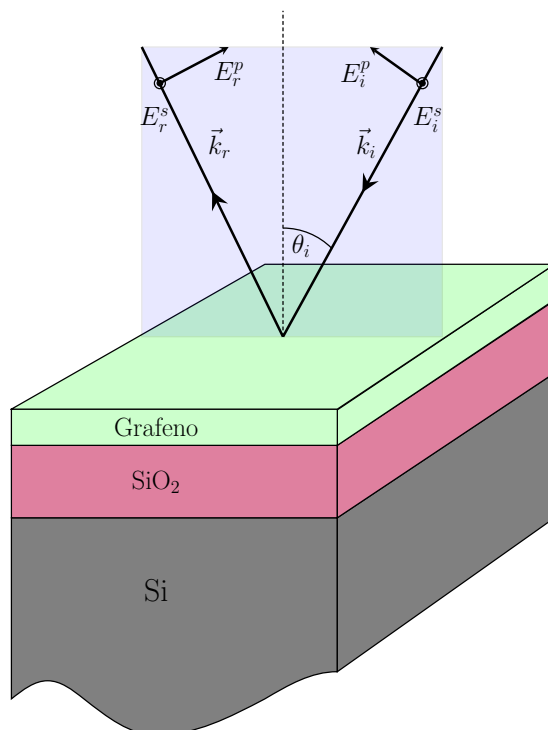


Figure 3.1: Carbon allotrope timeline

3.2 Graphene nanoribbons

3.2.1 Sample FG163R

3.2.2 Sample FG166L

3.2.3 Sample FG166R

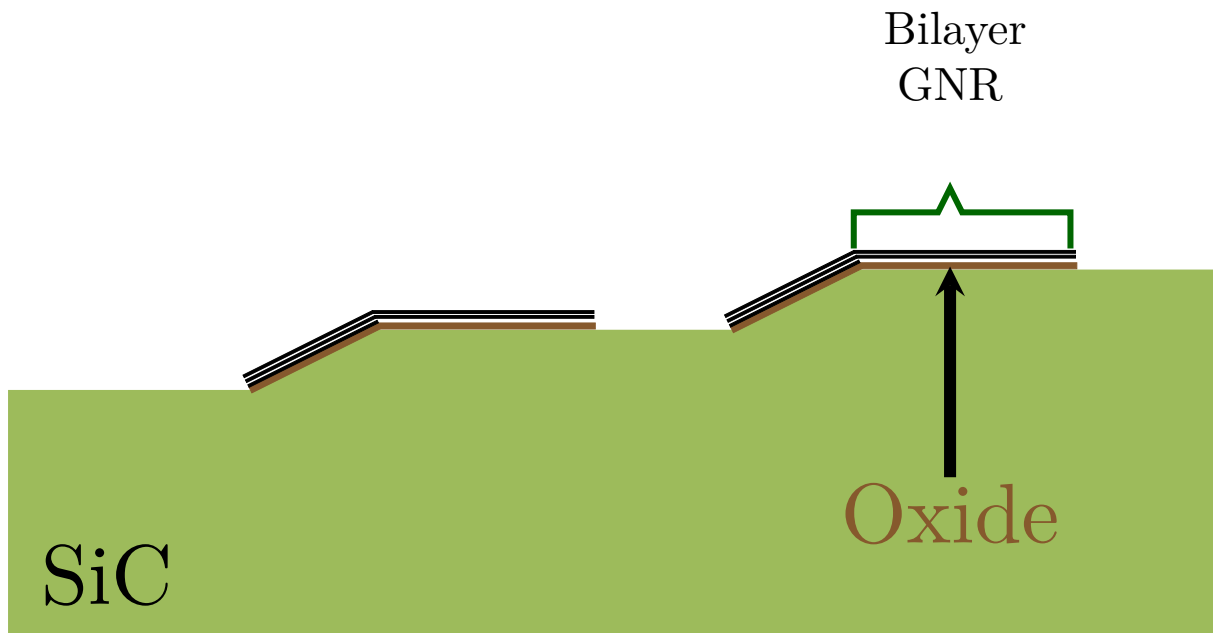


Figure 3.2: Carbon allotrope timeline

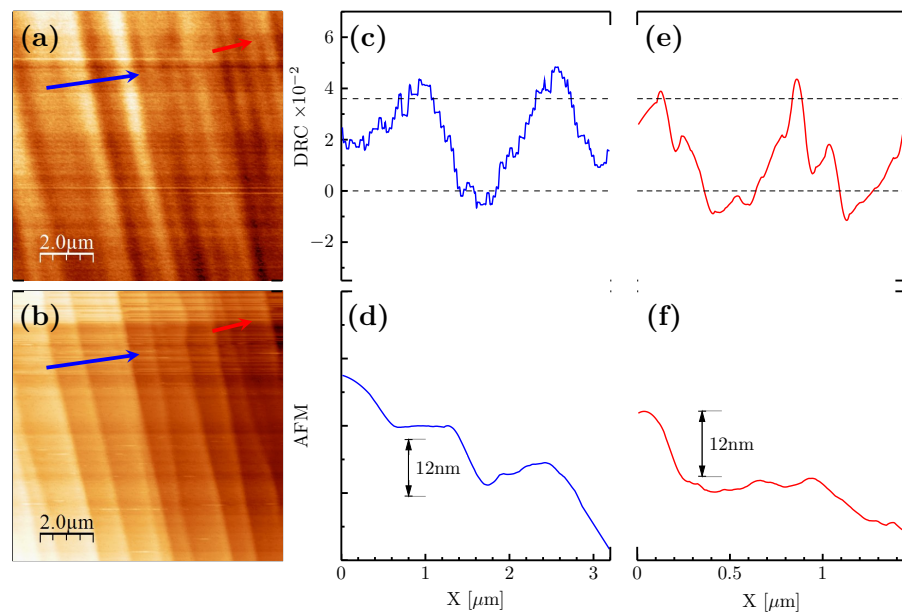


Figure 3.3: Carbon allotrope timeline

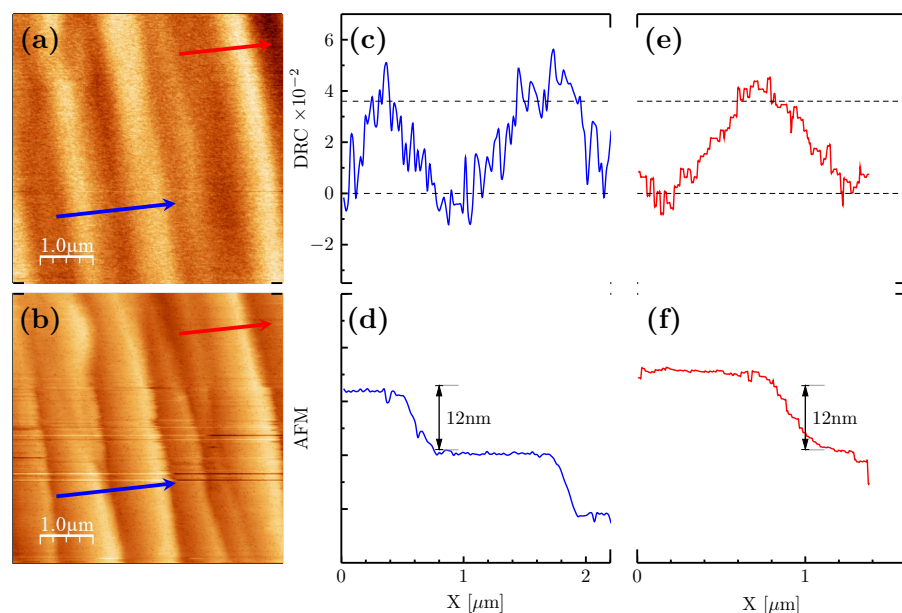


Figure 3.4: Carbon allotrope timeline

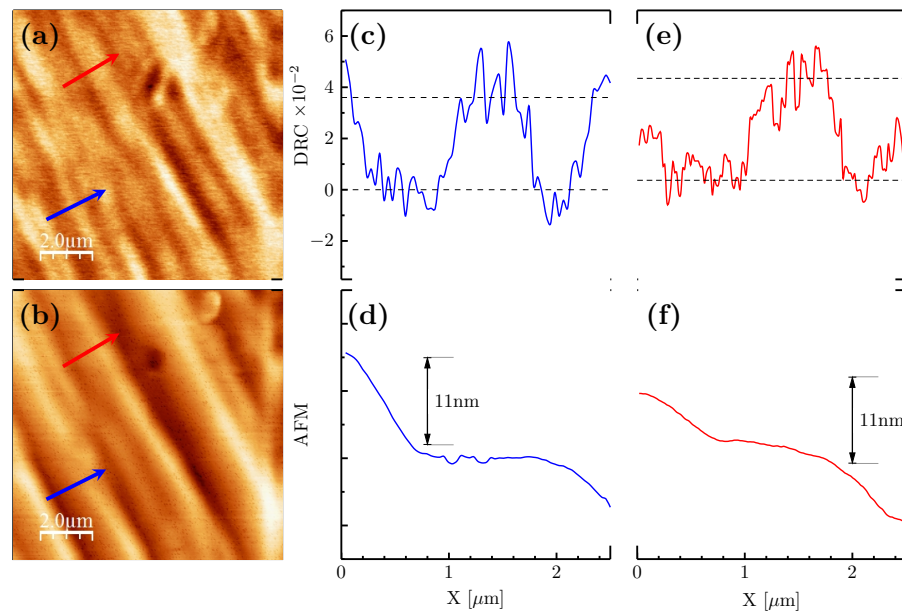


Figure 3.5: Carbon allotrope timeline

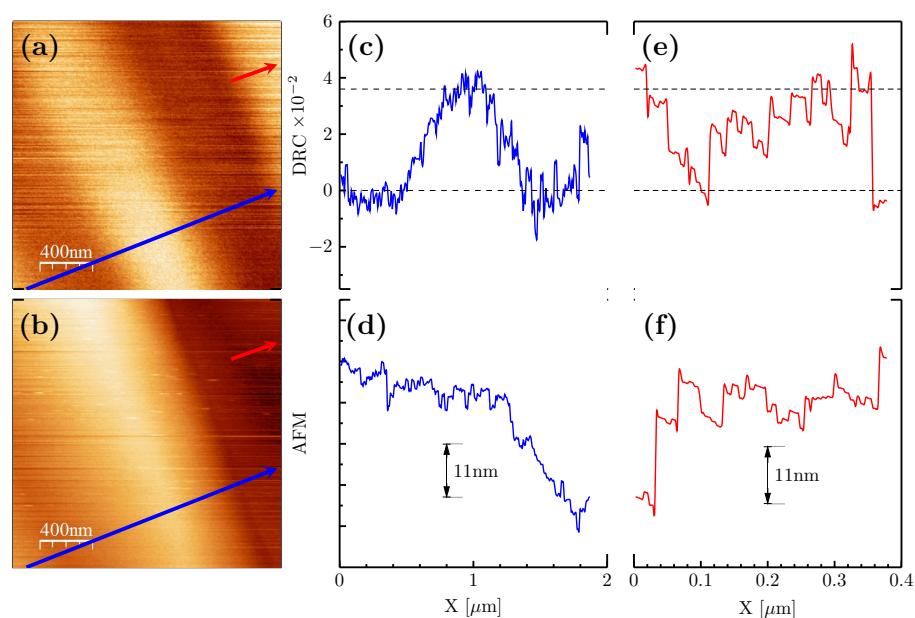


Figure 3.6: Carbon allotrope timeline

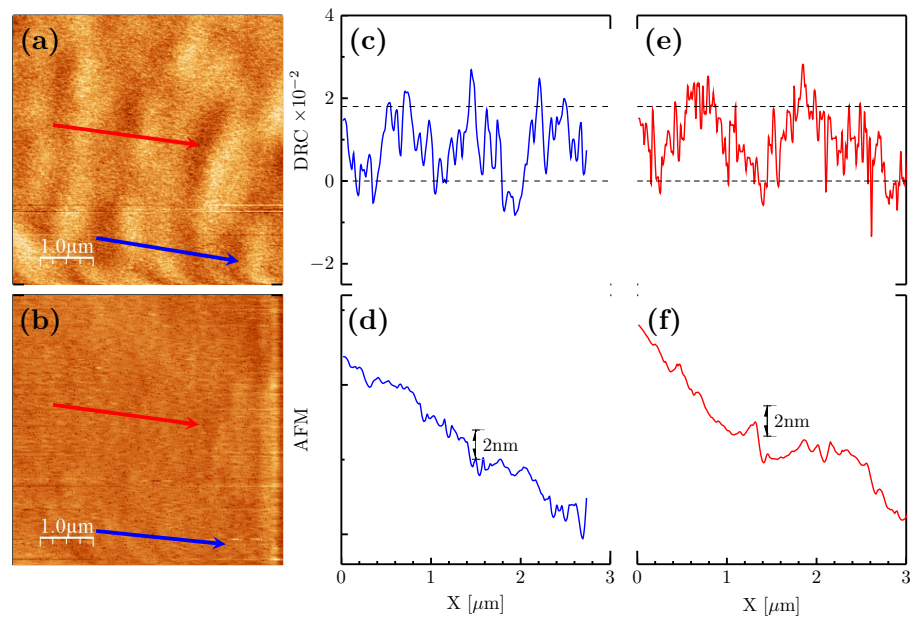


Figure 3.7: Carbon allotrope timeline

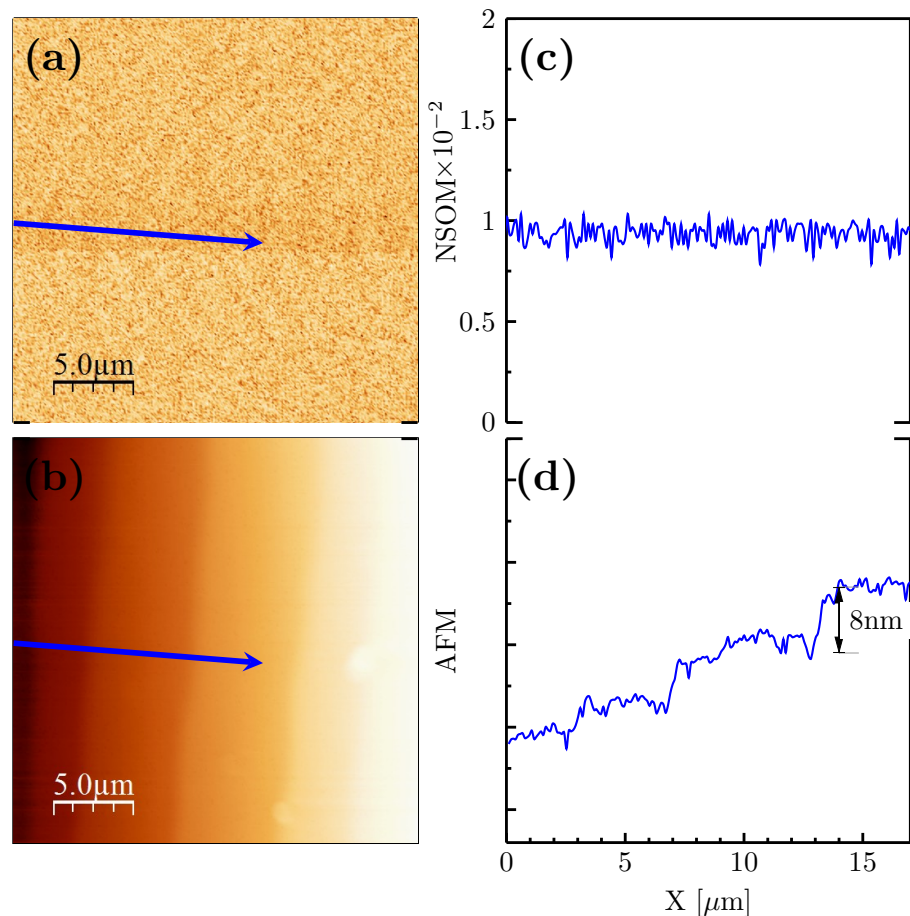


Figure 3.8: Carbon allotrope timeline

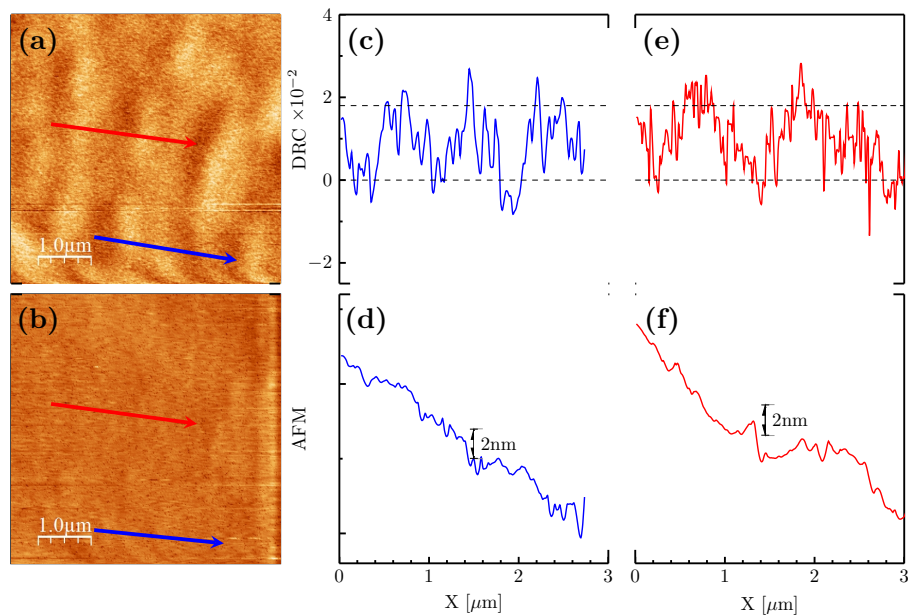


Figure 3.9: Carbon allotrope timeline

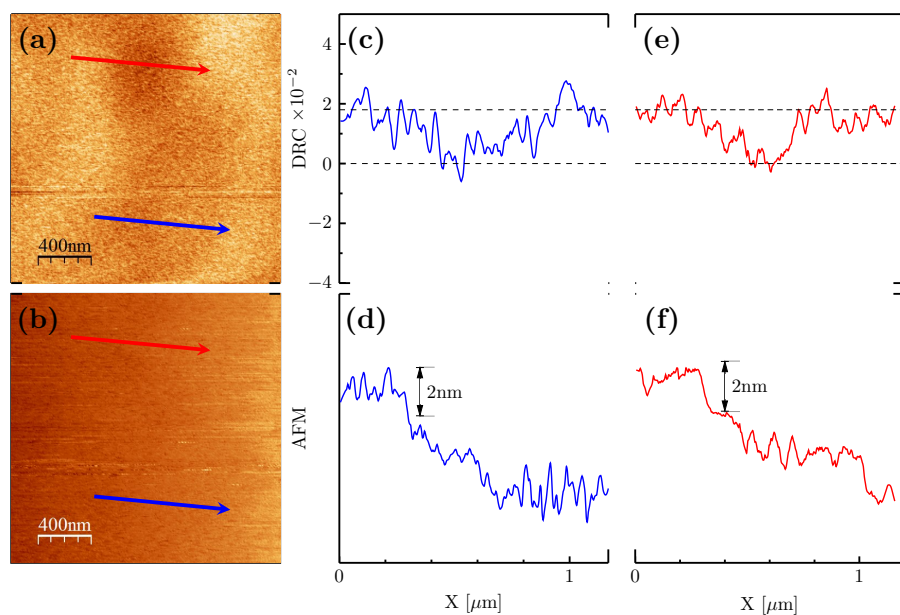


Figure 3.10: Carbon allotrope timeline

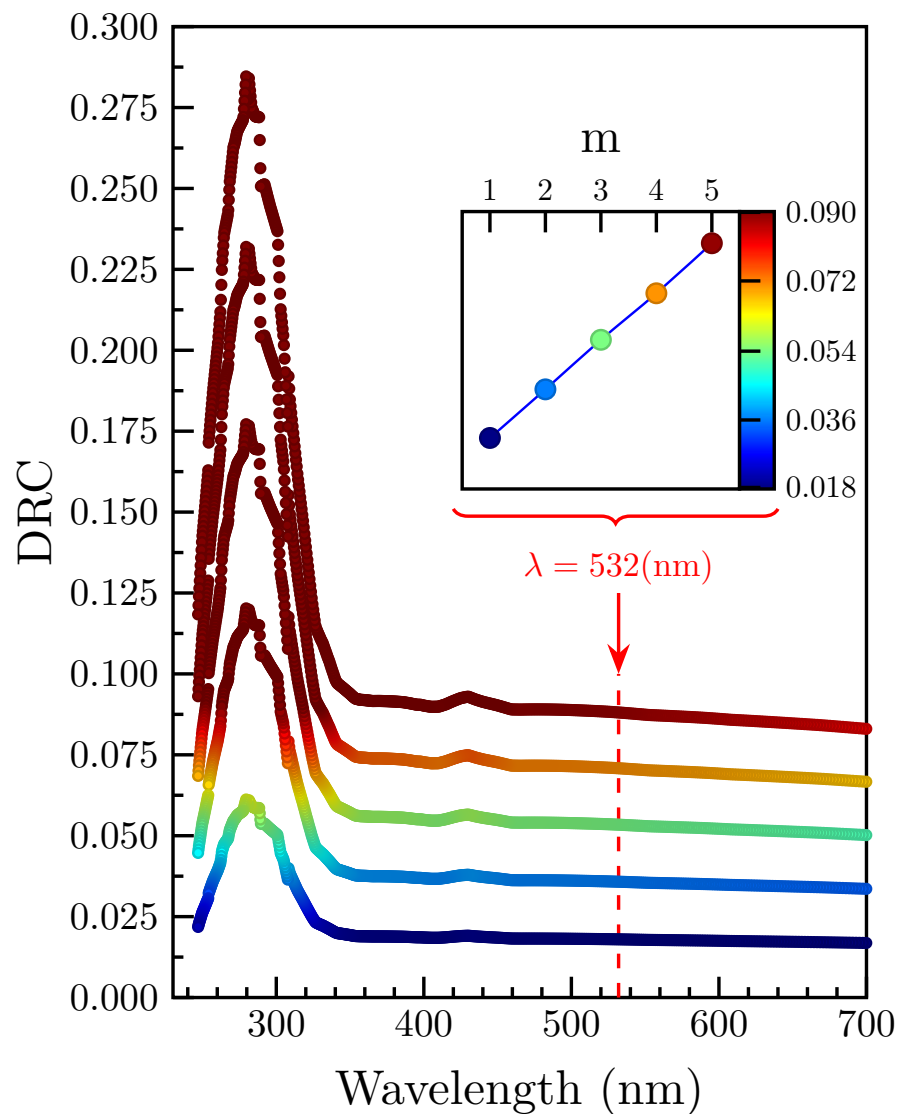


Figure 3.11: Carbon allotrope timeline

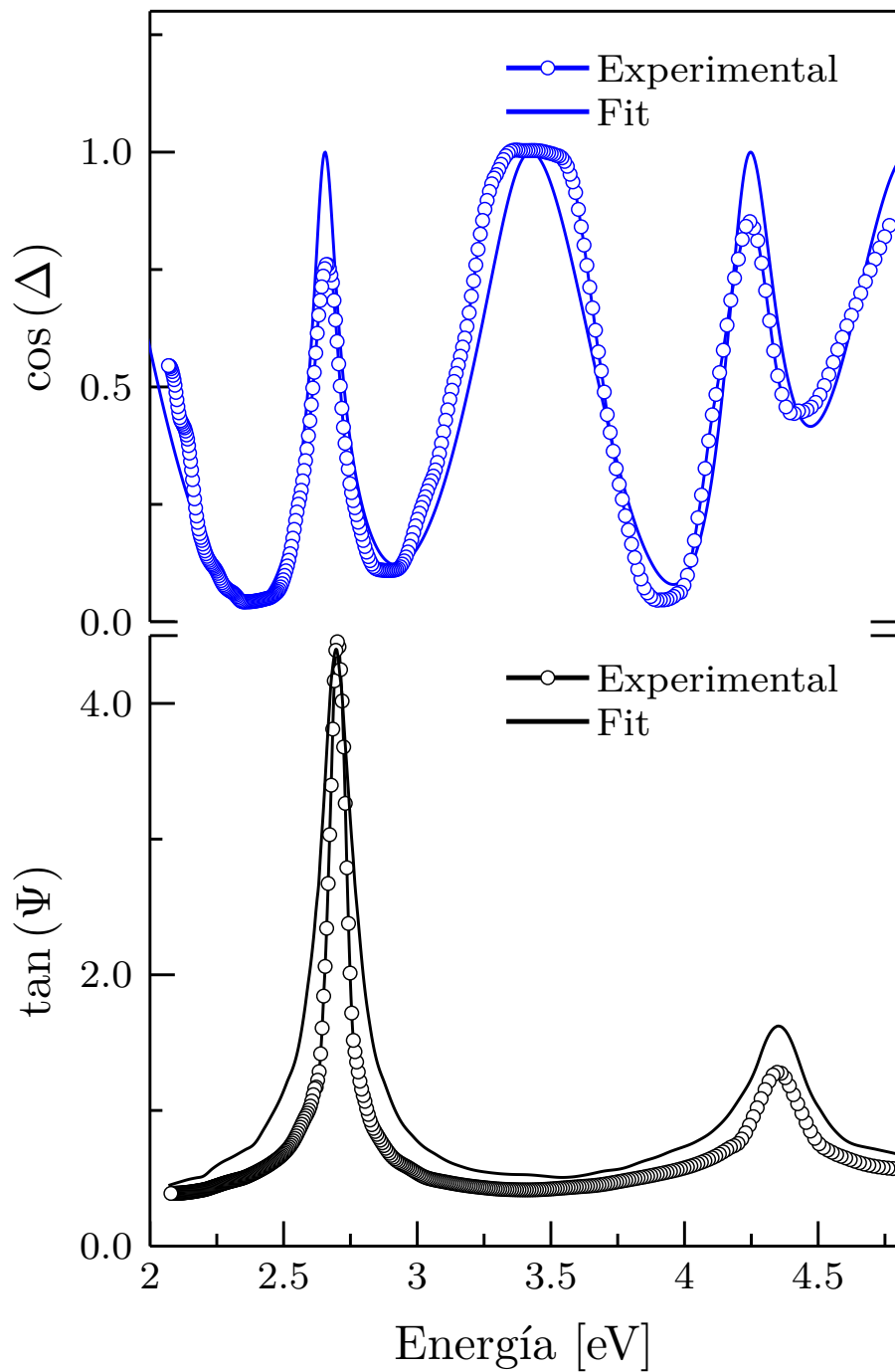


Figure 3.12: Carbon allotrope timeline



SAMPLES BASED CdTe

In this annex the results obtained from the modifications made on HgCdTe and CdTe samples are discussed. Mechanical modifications on the surface and silver evaporations were performed with the objective of understanding the behavior of a metal on a semiconductor. The idea of modifying the surfaces by evaporating was proposed, due to the intention of understanding in a fundamental way the novel materials known as topological insulators and given the particular phenomena that were presented in the HgCdTe quantum wells under considerations that will be addressed in this annex, the proposal is to study CdTe surfaces with Ag evaporations with the help of the e-beam coupled in the vacuum chamber.

Contents

A.1 Samples Descriptions	38
A.1.1 CdTe	38
A.1.2 ZnTe	38
A.1.3 CdZnTe	39
A.2 Results an Conclusions	44

The objective of the study by means of differential reflectance of the surface of HgCdT and of the materials of the CdTe family and especially CdTe with Ag evaporation is to reconstruct or to make a similarity of the surface position of the topological insulators, these materials that show properties of conductors in the surface and insulators in the bulk.

In first approximation this was implemented with the objective to know the surface of quantum wells of HgCdTe which show this behavior and it is due to the fact that in the walls the domains are stressed by the fact of the growth by MBE of this type of materials, for us a first approximation was to recreate in HgCdTe in bulk, small zones that would show stress and that we could monitor them by RDS, so the following was done:

1. In the HgCdTe sample using diamond paste we started to make in a preferential addition this carving or these surface modifications.
2. Evaporations of Ag which is a metal and we expect a similar behavior and that this will help us to compare what is the evolution when performing these treatments.

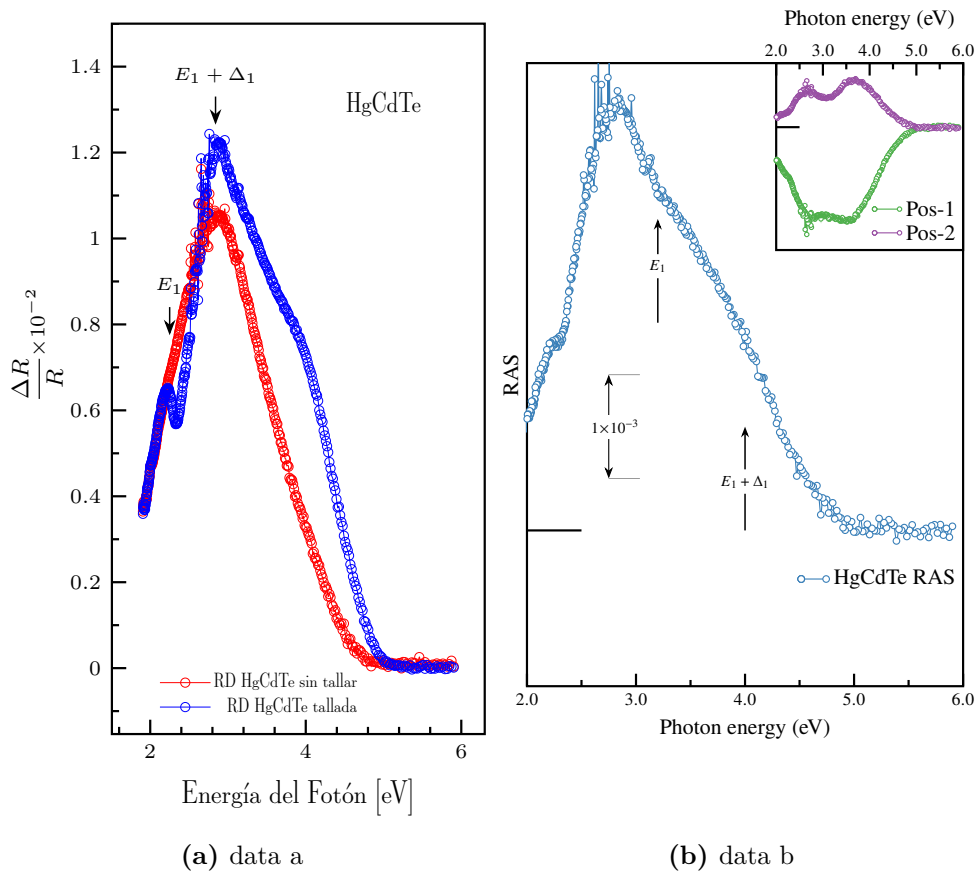
A.1 Samples Descriptions

	Description
Sample 01	CdTe
Sample 02	HgCdTe
Sample 03	HgCdTe
Sample 04	HgCdTe con superficie tallada
Sample 05	HgCdTe con superficie evaporada
Sample 06	CdZnTe

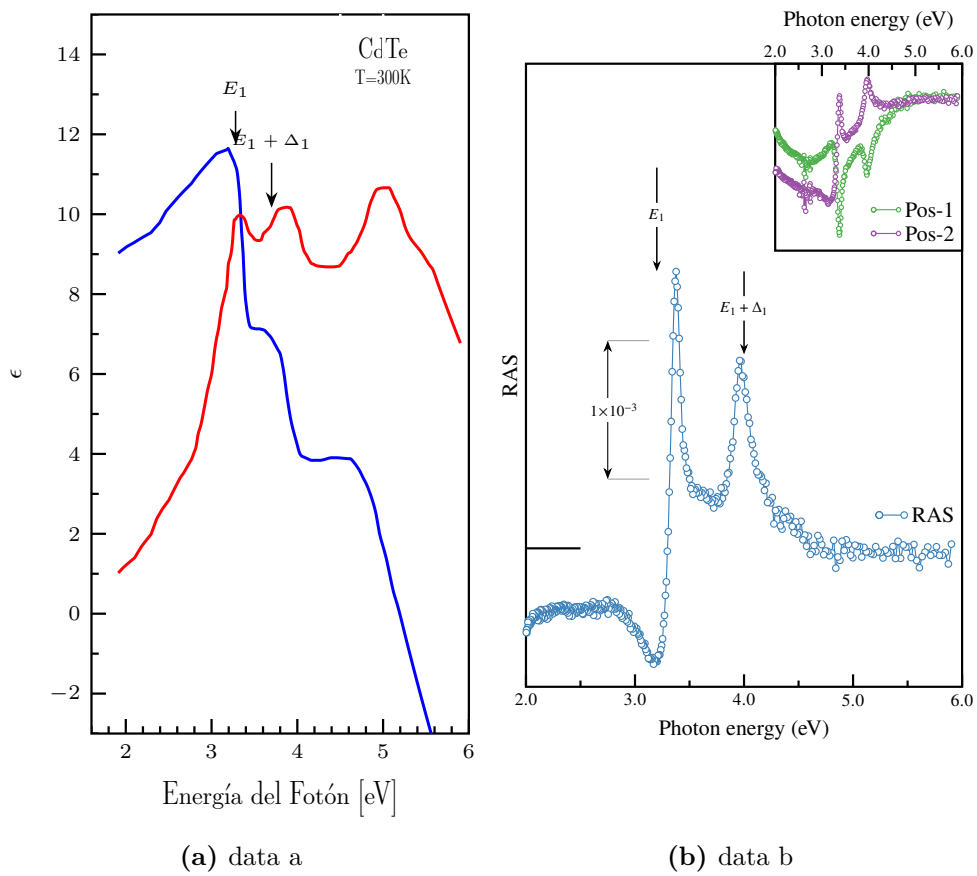
Table A.1: Samples studied from the *CdTe* family

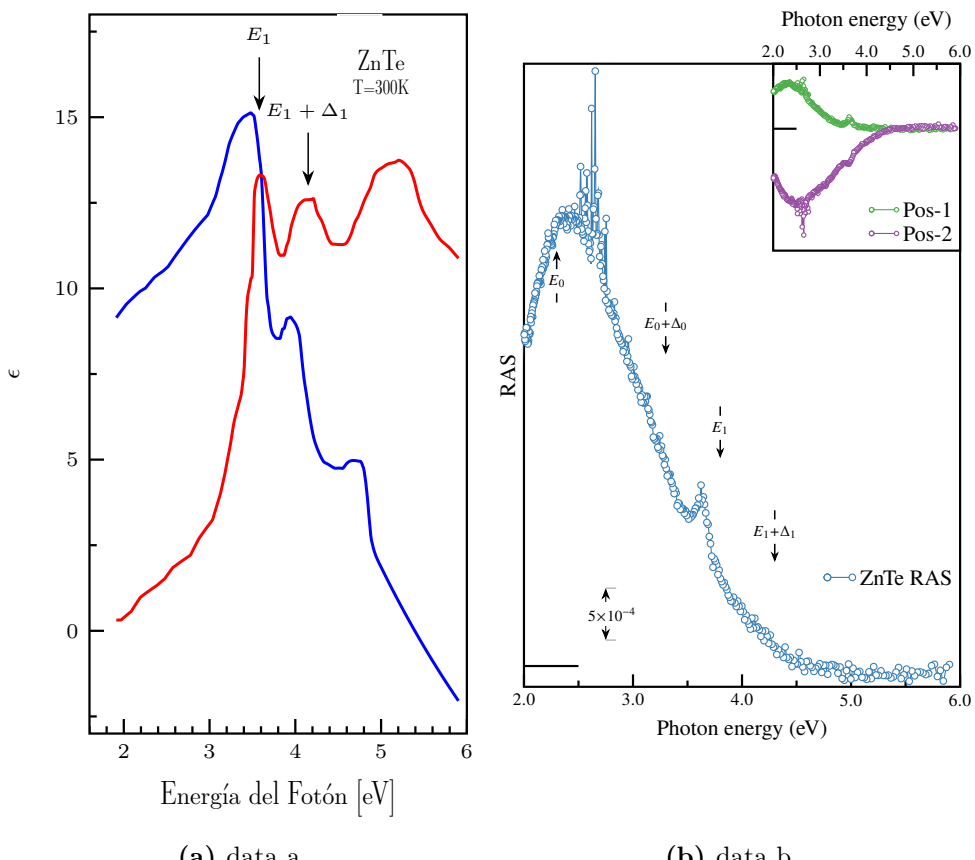
A.1.1 CdTe

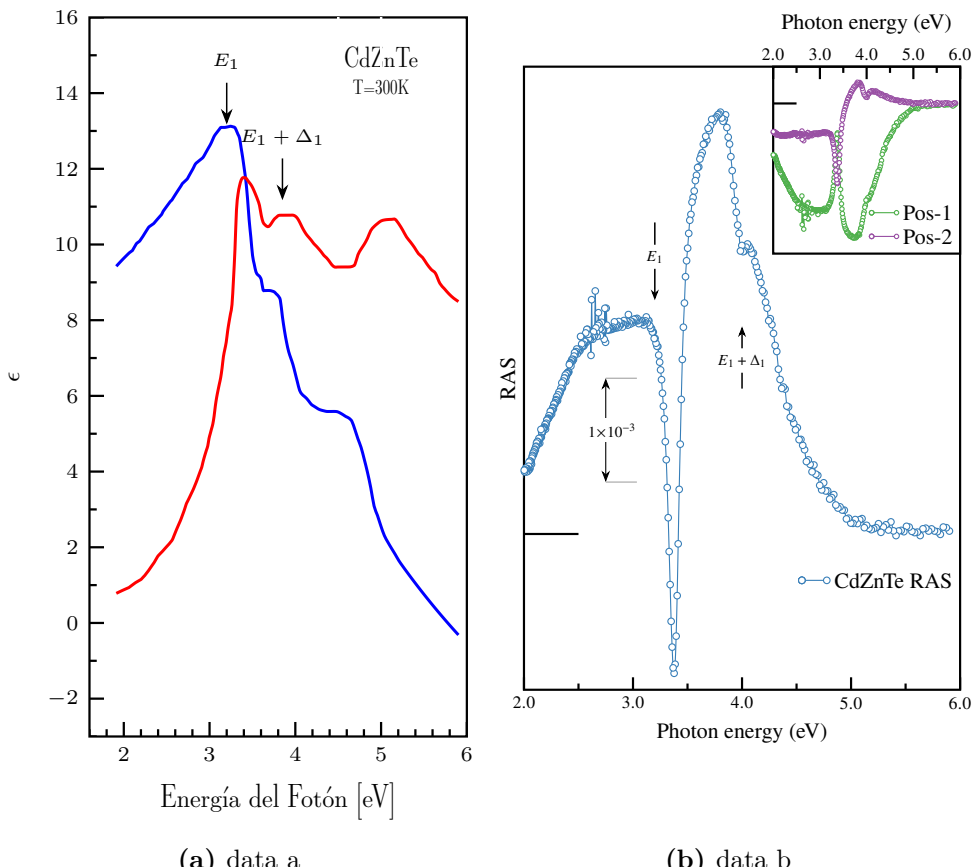
A.1.2 ZnTe

**Figure A.1:** all the data**A.1.3 CdZnTe**

En este apartado

**Figure A.2:** all the data

**Figure A.3:** all the data

**Figure A.4:** all the data

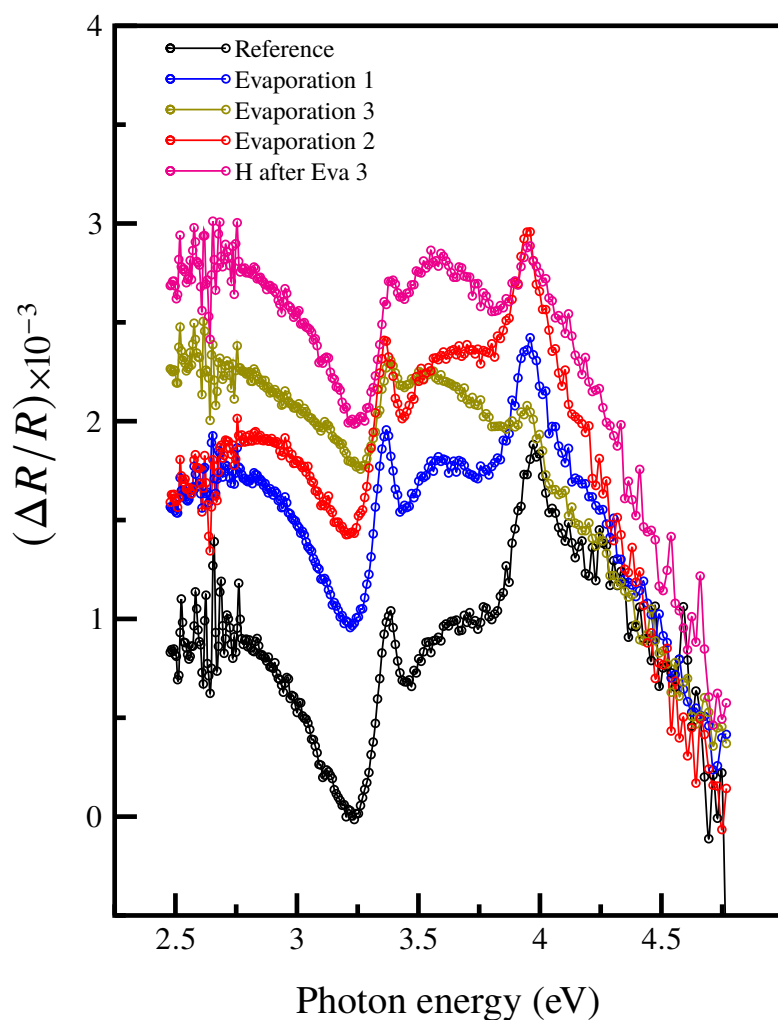
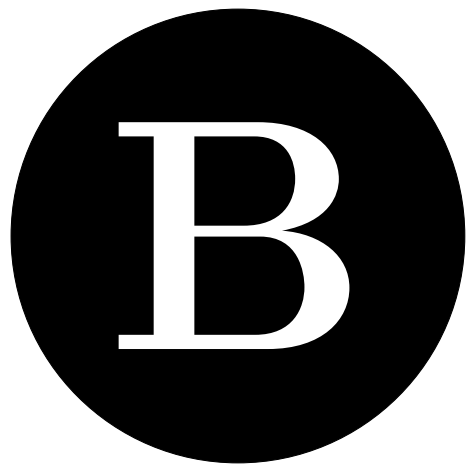


Figure A.5: Carbon allotrope timeline

A.2 Results an Conclusions

The evaporations were carried out with the e-beam performing the process of emptying the Ag material in the crucible, likewise the necessary treatment was given to the crucible so that it was in optimal cleaning conditions since the material previously contained was gadolinium.

One of the disadvantages when performing the evaporation of the material is that in literature this type of process comments that in several cases do not show a complete homogeneity in the evaporation of the same, this may be because the surface is not necessarily heated while evaporating, the temperature is not adequate and can be evaporated by drops, clusters, nanoparticles and even in so-called islands, in various works such as those of comments that under the conditions of heating the substrate and the distance at which it is located is quite optimal or likely to cover a wide area, so several evaporations were performed on the same sample and likewise several cases were monitored from the clean surface to the last evaporation and a reheated (this part is done because the area is more stable in terms of the surface), in conclusion the realiados processes were as follows.



SAMPLES CU₃N

Contents

B.1 Importance to study	46
B.2 Sample Descriptions	46
B.3 Results an Conclusions	47

B.1 Importance to study

B.2 Sample Descriptions

	Description
1 SLM	CuSn / Polymer (1cmx2.5xm)
2 SLM	CuSn / Polymer (1cmx2.5xm)
3 SLM	CuSn / Polymer (1cmx2.5xm)
4 SLM	CuSn / Polymer (1cmx2.5xm)
1 SLM+PP	CuSn / Polymer (1cmx2.5xm)
2 SLM+PP	CuSn / Polymer (1cmx2.5xm)
3 SLM+PP	CuSn / Polymer (1cmx2.5xm)
4 SLM+PP	CuSn / Polymer (1cmx2.5xm)

Table B.1: Description of 4 *CuSn* samples studied

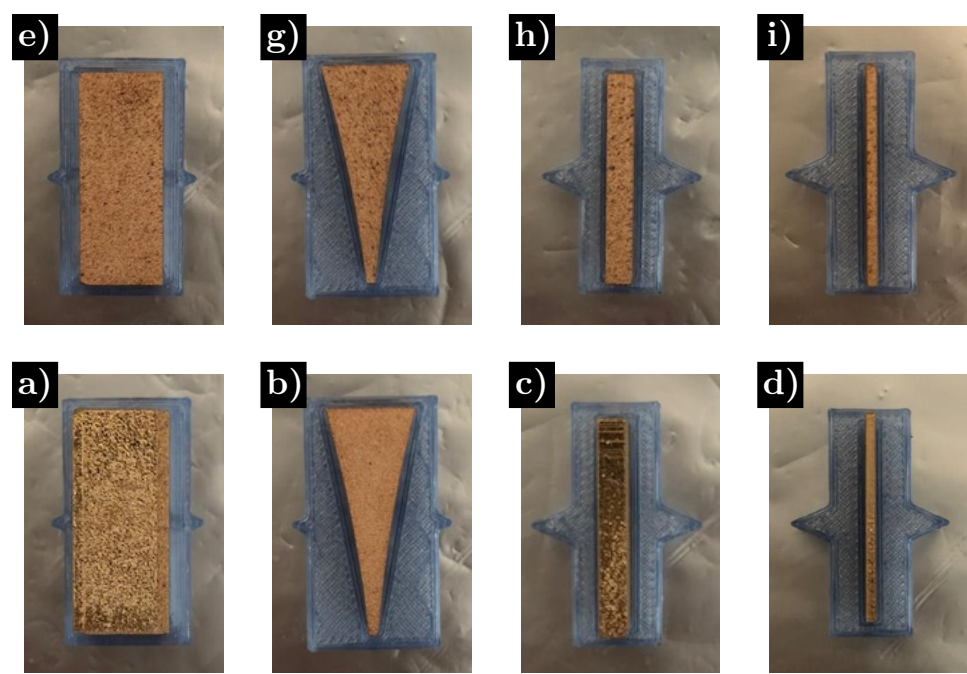


Figure B.1: Schematic diagram of graphene properties

B.3 Results an Conclusions

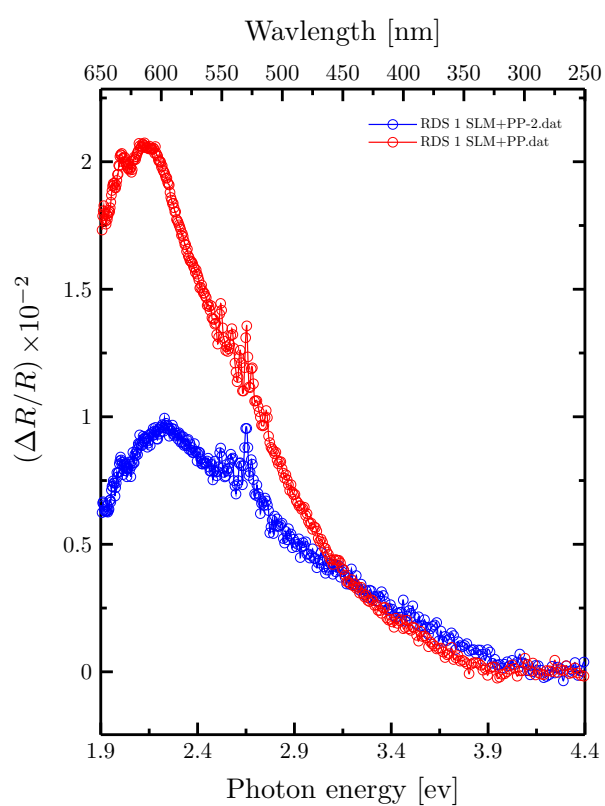


Figure B.2: RDS signal for the 1SLM+PP sample in different zones.

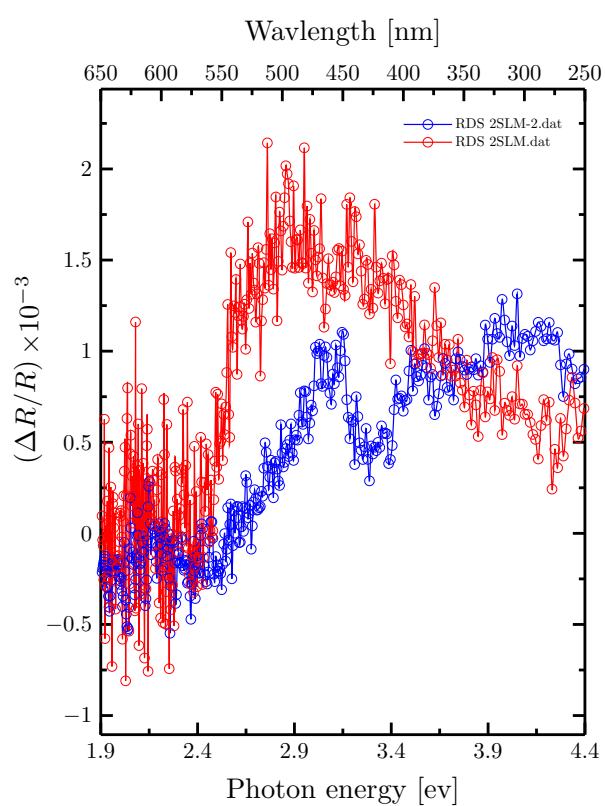


Figure B.3: RDS signal for the 2SLM sample in different zones.

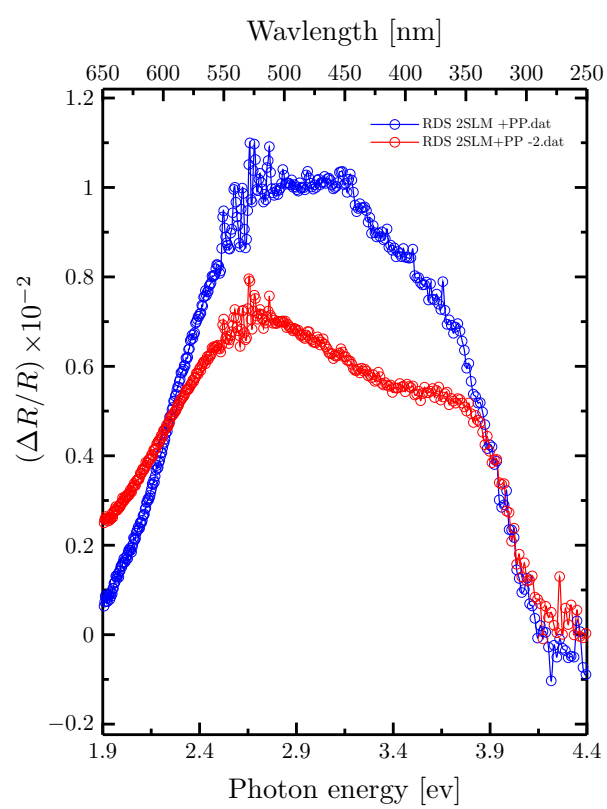


Figure B.4: RDS signal for the 2SLM+PP sample in different zones.

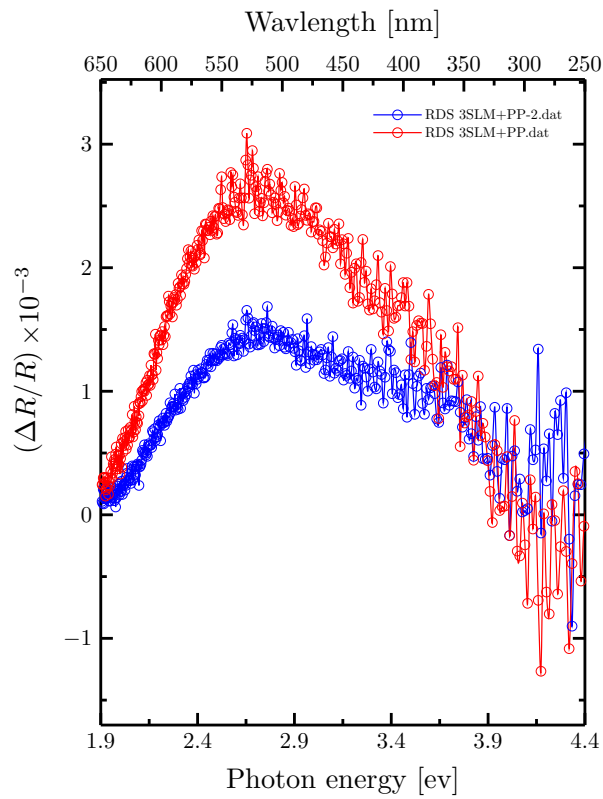


Figure B.5: RDS signal for the 3SLM+PP sample in different zones.

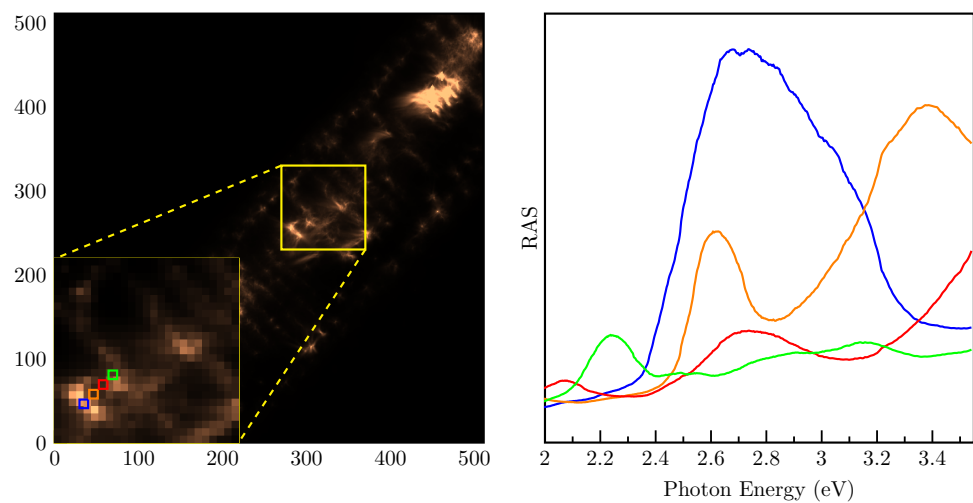
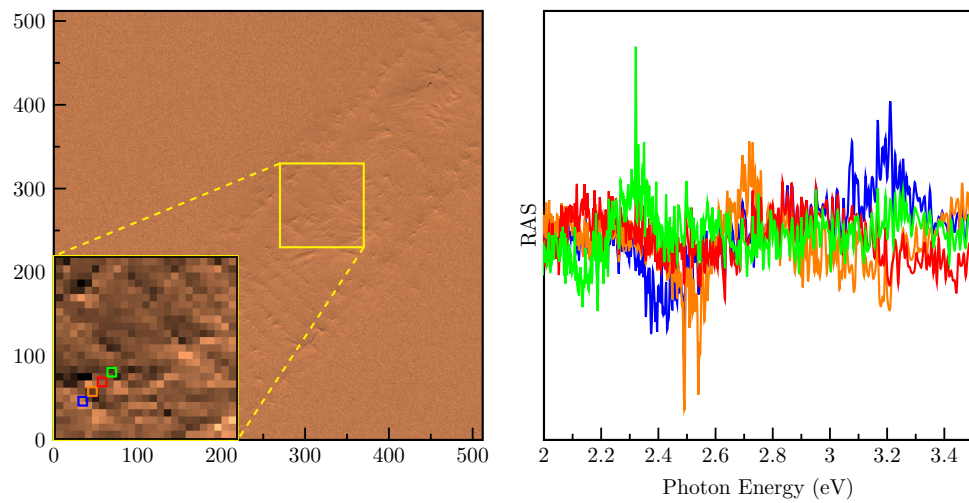
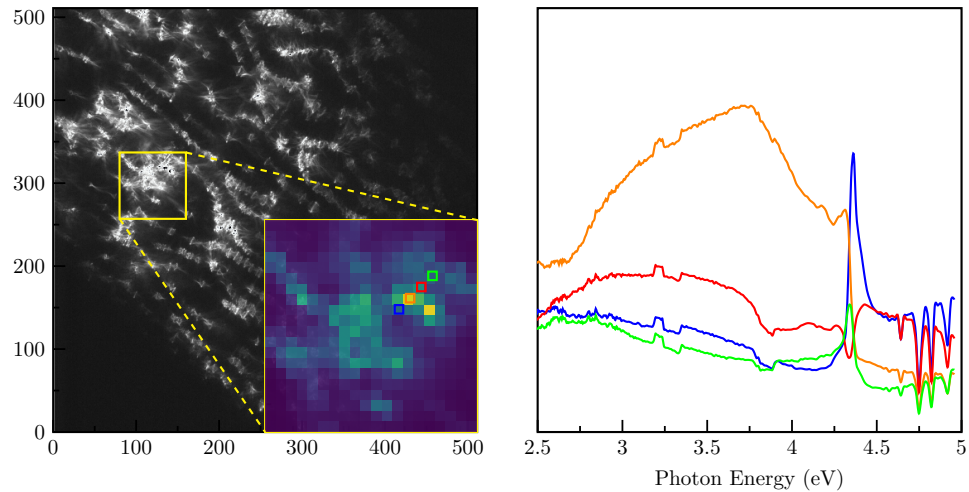
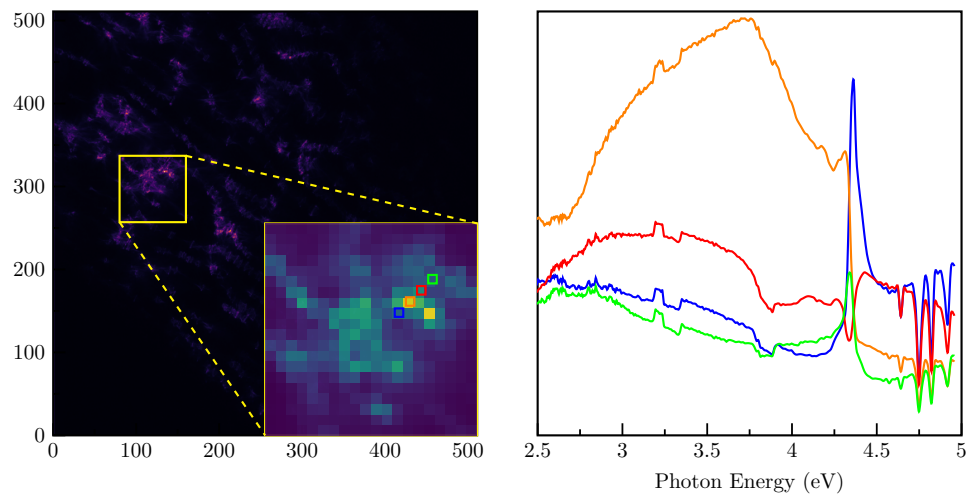


Figure B.6: Schematic diagram of graphene properties

**Figure B.7:** Schematic diagram of graphene properties**Figure B.8:** Schematic diagram of graphene properties**Figure B.9:** Schematic diagram of graphene properties

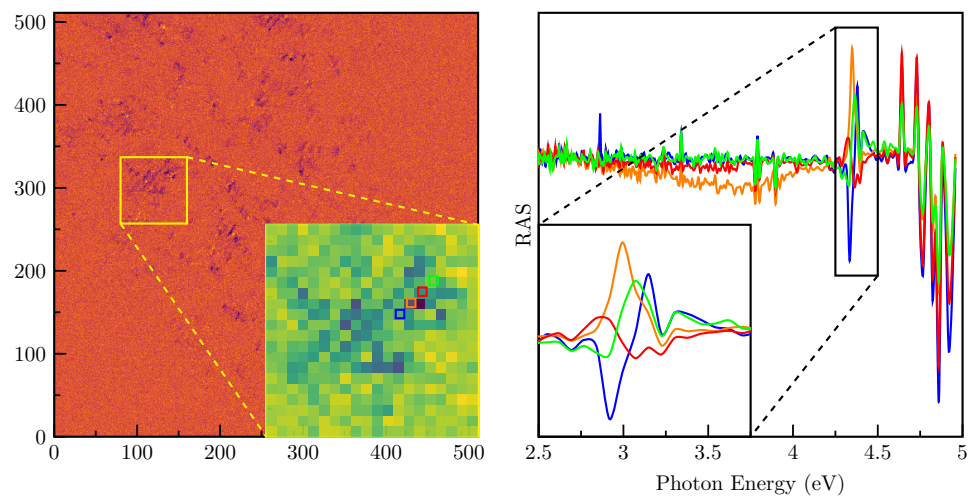


Figure B.10: Schematic diagram of graphene properties

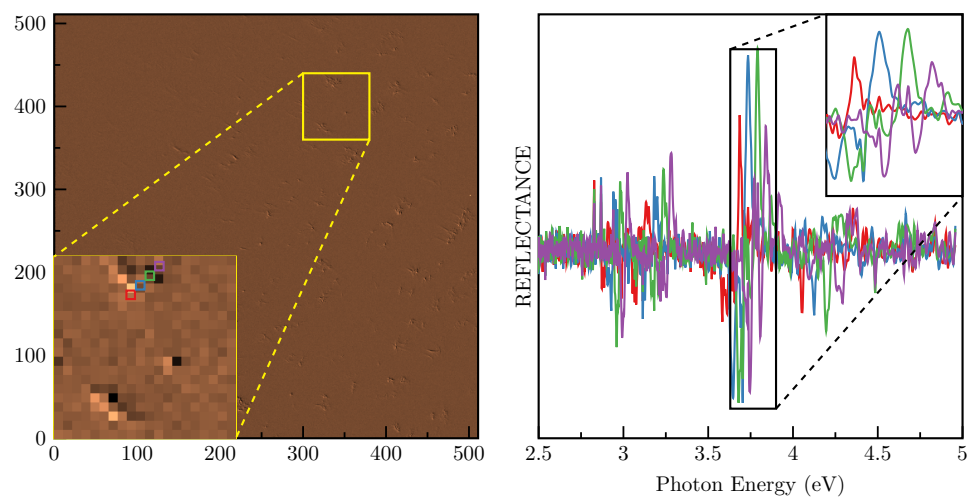
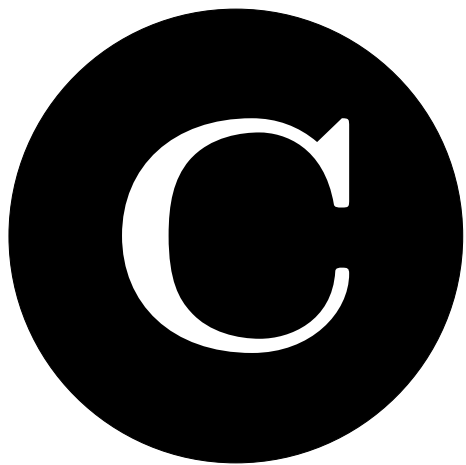


Figure B.11: Schematic diagram of graphene properties



INDUSTRY COLLABORATION

This appendix contains the Collaboration projects with Industry, these projects involves both experimental skills and programming to developed code for specific analysis.

Contents

C.1 Stratec project	55
C.2 Valeo project	58

C.1 Stratec project

This project developed by Nano photonics IICO's research group in collaboration with Sony-Stratec company was a preamble to contribute with research skills applied to industry. Without involves with industry devices developed, in this appendix we focus only on our contribution to solve a specific problem. This was consisted in the measure of depth into micro-devices composed by specific forms. The aim in this project basically consist in measure depth onto micro-devices, to get that measures we use the Micro Reflectance (μR) setup as shown in Figure C.1, where were measured each of these.

The monochromatic light incident on micro-device it generating multiple reflections, this allows to simulate the result spectra trough three-phase model [50]. Although, the optical alignment was a complex task, we reach measure around of 10 devices and analyze their results. To simplify the analysis, we developed a code which allowed to do a specific fit to get a more accuracy depth dimensions. Our code practically consist in developed a GUI (Graphical User Interface) to generate interacted fit, this in order to maximize and optimize the results.

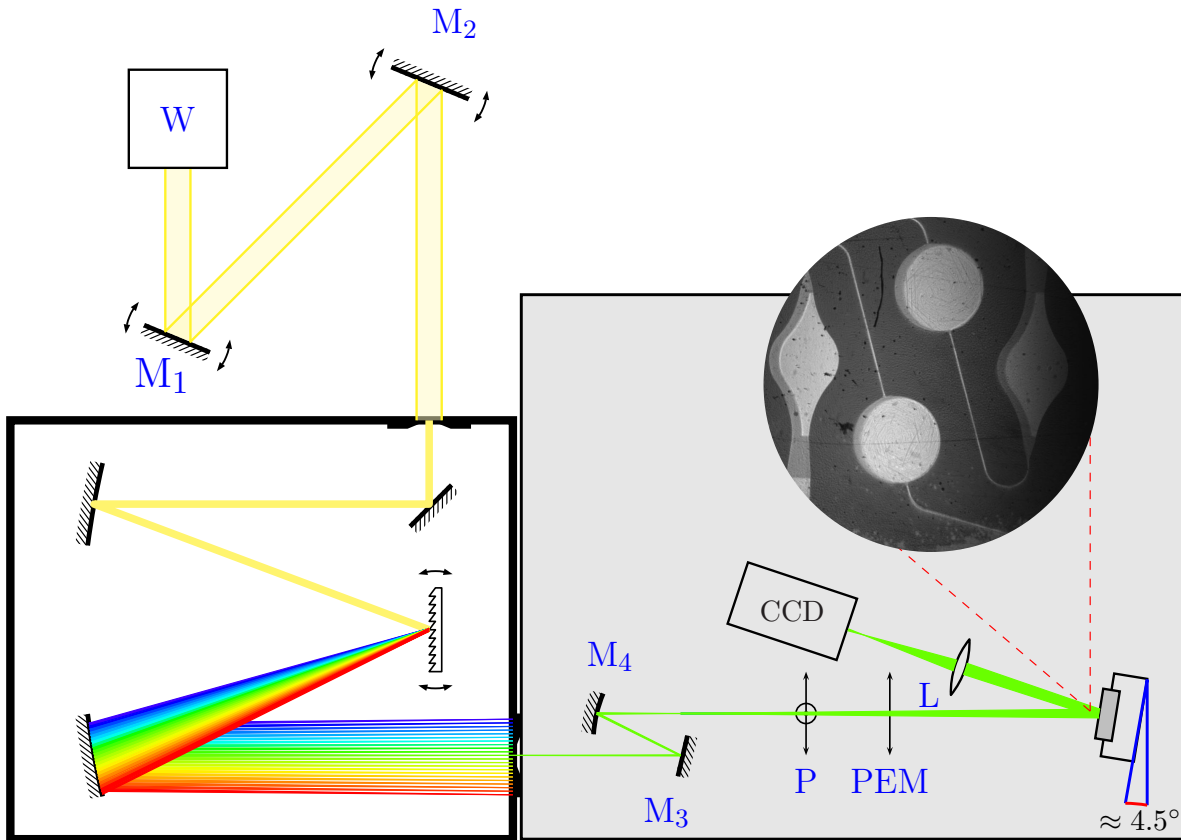


Figure C.1: Micro Reflectance setup into dark configuration.

C.1. Stratec project

56

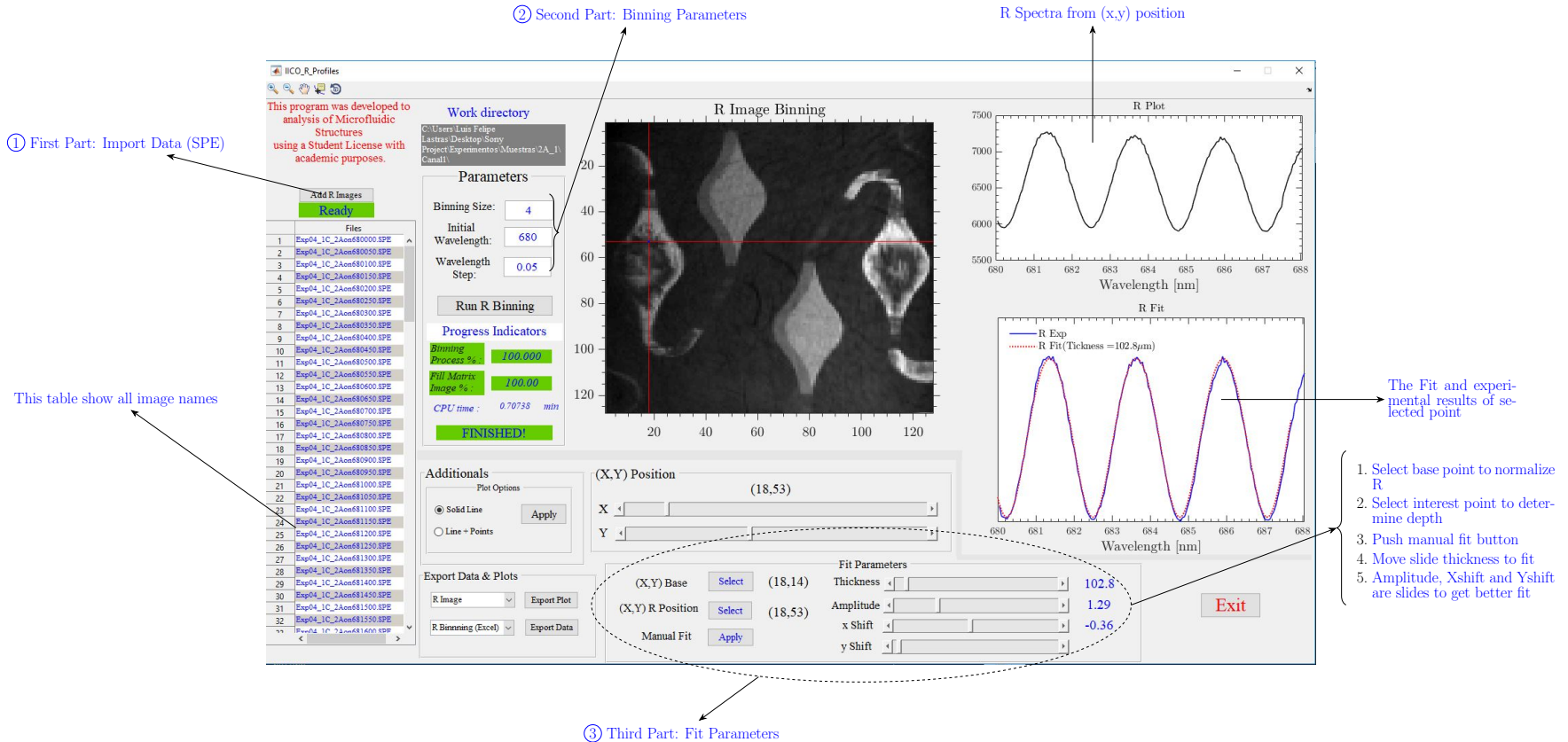


Figure C.2: GUI development to analysis.

Figure C.2 shown the GUI of developed code to result analysis. To use we need to upload all of CCD images to next apply a binning image process. Also, the interface have a user menu to choice the binning parameters, in this case we process all measures with a 4x4 binning. The central image map has a purpose the guide of image mapping pixel by pixel, this means if locate pointer on an any image pixel, it obtains the corresponding spectra, this, we allow a detailed analysis in specific zones. Already gets the binning process, as before mentioned we are proceeding to map with $x - y$ sliders, these help to position in specific pixel zone, this pixel return an R spectra, therefore we can apply the fit analysis through three-phase model proposed by L.F Lastras Martínez *et al.* [50].

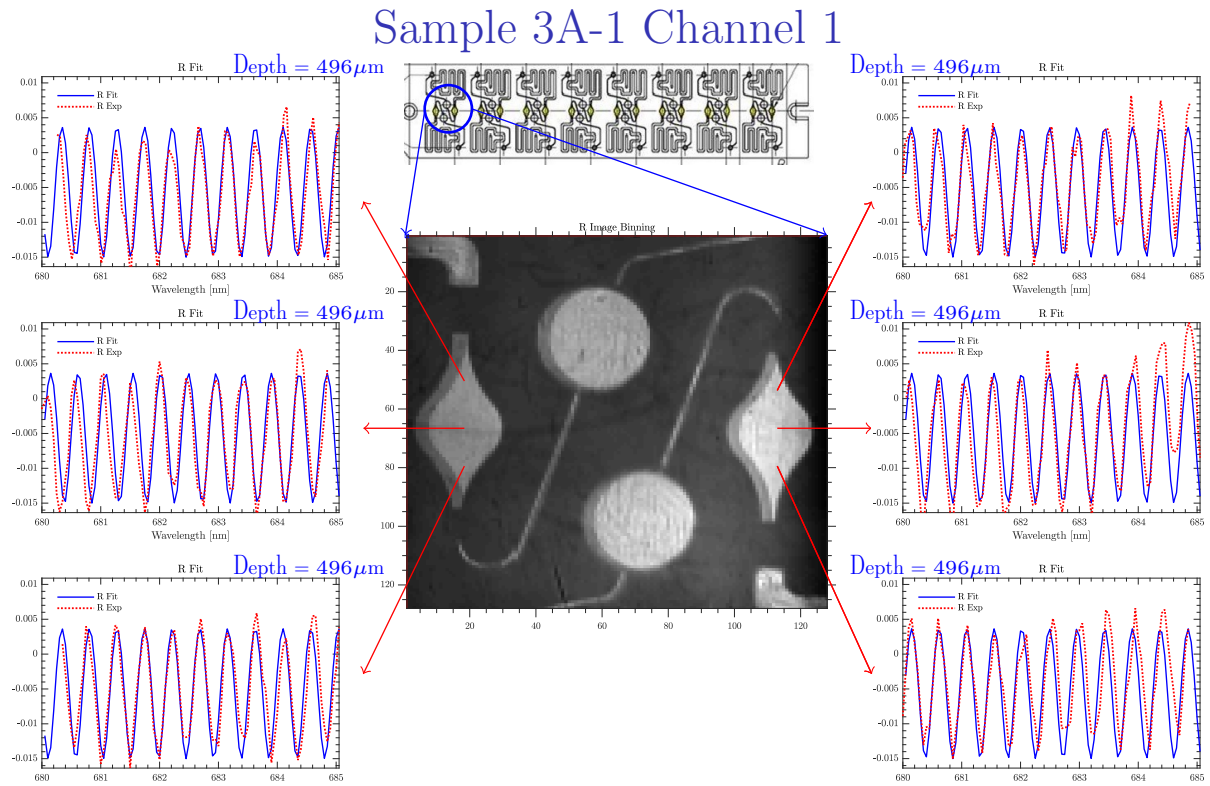


Figure C.3: Image analysis of micro-device measure, at top locate the diagram of this device, where the study zone is enclosing. At center shown an image measured inside the spectral range with the marks of analyzed zones. Finally, at both sides the corresponding spectral results of each analyzed zones, in each of these denotes the depth result obtained through the fit.

The results obtained were satisfactory in order to attendance the industry requirements, leaving us a gratifying collaboration experience with industry.

C.2 Valeo project

In this project as the previous project we focus on a general explanation in our work realized in it. Our task was the characterization of mechanical wear in a blade. The characterization were carried out trough three systems: confocal optical microscope, metallographic microscope and profilometer. These blades were consisted in three shapes; the aim was to measure mechanical wear in this cutting tools, focused on specif zones.

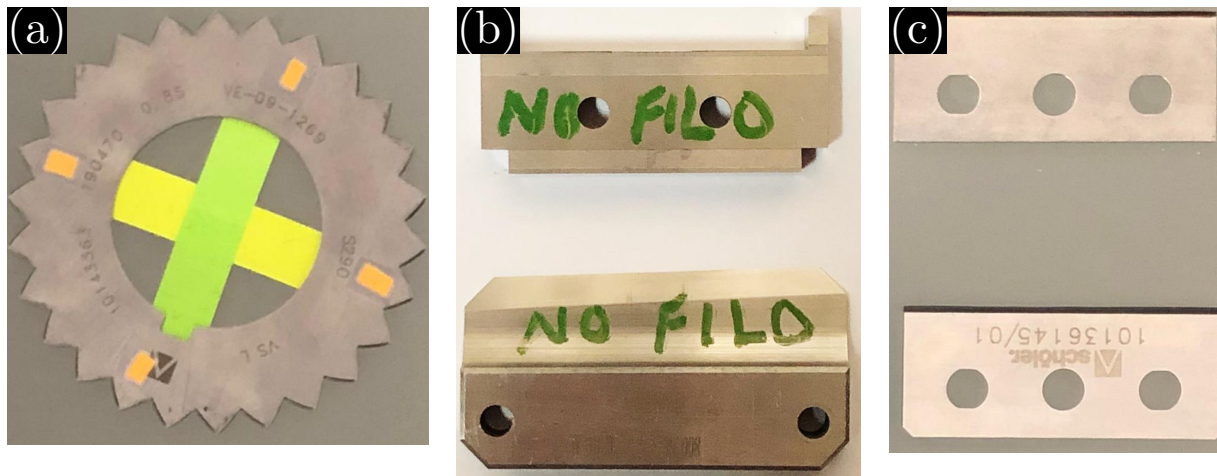


Figure C.4: Three shapes of characterized samples.

BIBLIOGRAPHY

- [1] L. Aranha Galves. Fabrication and characterization of graphene nanoribbons epitaxially grown on sic (0001). 2018. (Cited on page 25.)
- [2] P. Avouris and C. Dimitrakopoulos. Graphene: synthesis and applications. *Materials today*, 15(3):86–97, 2012. (Not cited.)
- [3] R. M. Azzam, N. M. Bashara, and S. S. Ballard. Ellipsometry and polarized light. *Physics Today*, 31(11):72, 1978. (Cited on page 19.)
- [4] J. A. Badán. Caracterización óptica de materiales luz polarizada y nanoestructuras. 2014. (Not cited.)
- [5] S. A. Bansal, A. P. Singh, and S. Kumar. 2d materials: Graphene and others. In *AIP Conference Proceedings*, volume 1728, page 020459. AIP Publishing LLC, 2016. (Not cited.)
- [6] J. Baringhaus, J. Aprojanz, J. Wiegand, D. Laube, M. Halbauer, J. Hübner, M. Oestreich, and C. Tegenkamp. Growth and characterization of sidewall graphene nanoribbons. *Applied Physics Letters*, 106(4):043109, 2015. (Not cited.)
- [7] J. Baringhaus, M. Ruan, F. Edler, A. Tejeda, M. Sicot, A. Taleb-Ibrahimi, A.-P. Li, Z. Jiang, E. H. Conrad, C. Berger, et al. Exceptional ballistic transport in epitaxial graphene nanoribbons. *Nature*, 506(7488):349–354, 2014. (Cited on page 5.)
- [8] V. Barone, O. Hod, and G. E. Scuseria. Electronic structure and stability of semiconducting graphene nanoribbons. *Nano letters*, 6(12):2748–2754, 2006. (Not cited.)
- [9] G. Binnig, C. F. Quate, and C. Gerber. Atomic force microscope. *Physical review letters*, 56(9):930, 1986. (Cited on page 24.)
- [10] G. Binnig, H. Rohrer, C. Gerber, and E. Weibel. Surface studies by scanning tunneling microscopy. *Physical review letters*, 49(1):57, 1982. (Cited on page 24.)
- [11] P. E. Blöchl. Projector augmented-wave method. *Phys. Rev. B*, 50:17953–17979, Dec 1994. (Cited on pages 10 and 12.)
- [12] J. J. Brouillet. *Graphene-Mediated Light-Matter Interaction*. PhD thesis, California Institute of Technology, 2019. (Not cited.)
- [13] L. C. Campos, V. R. Manfrinato, J. D. Sanchez-Yamagishi, J. Kong, and P. Jarillo-Herrero. Anisotropic etching and nanoribbon formation in single-layer graphene. *Nano Letters*, 9(7):2600–2604, Jul 2009. (Cited on page 9.)

- [14] L. Cao and K. Sendur. Surface roughness effects on the broadband reflection for refractory metals and polar dielectrics. *Materials*, 12(19):3090, 2019. (Not cited.)
- [15] Y. Cao, V. Fatemi, A. Demir, S. Fang, S. L. Tomarken, J. Y. Luo, J. D. Sanchez-Yamagishi, K. Watanabe, T. Taniguchi, E. Kaxiras, R. C. Ashoori, and P. Jarillo-Herrero. Correlated insulator behaviour at half-filling in magic-angle graphene superlattices. *Nature*, 556(7699):80–84, Apr 2018. (Cited on page 9.)
- [16] Y. Cao, V. Fatemi, S. Fang, K. Watanabe, T. Taniguchi, E. Kaxiras, and P. Jarillo-Herrero. Unconventional superconductivity in magic-angle graphene superlattices. *Nature*, 556(7699):43–50, 2018. (Cited on page 9.)
- [17] M. Cardona and Y. Y. Peter. *Fundamentals of semiconductors*, volume 619. Springer, 2005. (Cited on pages X and 18.)
- [18] A. Celis, M. N. Nair, A. Taleb-Ibrahimi, E. Conrad, C. Berger, W. De Heer, and A. Tejeda. Graphene nanoribbons: fabrication, properties and devices. *Journal of Physics D: Applied Physics*, 49(14):143001, 2016. (Cited on page 5.)
- [19] W. K. Chee, H. N. Lim, Z. Zainal, N. M. Huang, I. Harrison, and Y. Andou. Flexible graphene-based supercapacitors: a review. *The Journal of Physical Chemistry C*, 120(8):4153–4172, 2016. (Cited on page 5.)
- [20] J. Chen, M. Badioli, P. Alonso-González, S. Thongrattanasiri, F. Huth, J. Osmond, M. Spasenović, A. Centeno, A. Pesquera, P. Godignon, et al. Optical nano-imaging of gate-tunable graphene plasmons. *Nature*, 487(7405):77–81, 2012. (Not cited.)
- [21] L. Chong, H. Guo, Y. Zhang, Y. Hu, and Y. Zhang. Raman study of strain relaxation from grain boundaries in epitaxial graphene grown by chemical vapor deposition on sic. *Nanomaterials*, 9(3):372, 2019. (Not cited.)
- [22] J. Cleveland, B. Anczykowski, A. Schmid, and V. Elings. Energy dissipation in tapping-mode atomic force microscopy. *Applied Physics Letters*, 72(20):2613–2615, 1998. (Cited on page 25.)
- [23] A. Cricenti, G. Longo, M. Luce, R. Generosi, P. Perfetti, D. Vobornik, G. Margaritondo, P. Thielen, J. Sanghera, I. Aggarwal, et al. Afm and snom characterization of carboxylic acid terminated silicon and silicon nitride surfaces. *Surface science*, 544(1):51–57, 2003. (Cited on pages 24 and 25.)
- [24] J. Dilts. Design, fabrication, and characterization of multilayer hyperbolic metamaterials. 2019. (Not cited.)
- [25] P. Eaton and P. West. *Atomic force microscopy*. Oxford university press, 2010. (Cited on page 25.)

- [26] J. Enkovaara, C. Rostgaard, J. J. Mortensen, J. Chen, M. Dułak, L. Ferrighi, J. Gavnholt, C. Glinsvad, V. Haikola, H. A. Hansen, H. H. Kristoffersen, M. Kuisma, A. H. Larsen, L. Lehtovaara, M. Ljungberg, O. Lopez-Acevedo, P. G. Moses, J. Ojanen, T. Olsen, V. Petzold, N. A. Romero, J. Stausholm-Møller, M. Strange, G. A. Tritsaris, M. Vanin, M. Walter, B. Hammer, H. Häkkinen, G. K. H. Madsen, R. M. Nieminen, J. K. Nørskov, M. Puska, T. T. Rantala, J. Schiøtz, K. S. Thygesen, and K. W. Jacobsen. Electronic structure calculations with GPAW: a real-space implementation of the projector augmented-wave method. *Journal of Physics: Condensed Matter*, 22(25):253202, jun 2010. (Cited on pages 10 and 12.)
- [27] G. Flores-Rangel, L. Lastras-Martínez, R. Castro-García, O. Ruiz-Cigarrillo, R. Balderas-Navarro, L. Espinosa-Cuellar, A. Lastras-Martínez, and J. Lopes. Optical contrast in the near-field limit for structural characterization of graphene nanoribbons. *Applied Surface Science*, 536:147710, 2021. (Cited on page 6.)
- [28] H. Fujiwara. *Spectroscopic ellipsometry: principles and applications*. John Wiley & Sons, 2007. (Cited on pages 19 and 20.)
- [29] H. Furukawa and S. Kawata. Analysis of image formation in a near-field scanning optical microscope: effects of multiple scattering. *Optics communications*, 132(1-2):170–178, 1996. (Not cited.)
- [30] D. Galpaya. *Synthesis, characterization and applications of graphene oxide-polymer nanocomposites*. PhD thesis, Queensland University of Technology, 2015. (Not cited.)
- [31] M. H. Gass, U. Bangert, A. L. Bleloch, P. Wang, R. R. Nair, and A. Geim. Free-standing graphene at atomic resolution. *Nature nanotechnology*, 3(11):676–681, 2008. (Not cited.)
- [32] F. J. Giessibl. Advances in atomic force microscopy. *Reviews of modern physics*, 75(3):949, 2003. (Cited on page 24.)
- [33] GPAW. Gpaw code, 2020. (Cited on page VIII.)
- [34] P. Graves and D. Gardiner. Practical raman spectroscopy. *Springer*, 1989. (Not cited.)
- [35] M. Grundmann. *Physics of semiconductors*, volume 11. Springer, 2010. (Not cited.)
- [36] J. W. Guikema. *Scanning Hall probe microscopy of magnetic vortices in very underdoped yttrium-barium-copper-oxide*. PhD thesis, stanford university, 2004. (Not cited.)
- [37] Y. Gupta and P. Arun. First step to ellipsometry. *International Journal of Physics*, 3(1):8–11, 2015. (Not cited.)

- [38] O. S. Heavens. *Optical properties of thin solid films*. Courier Corporation, 1991. (Not cited.)
- [39] K. Hingerl, R. Balderas-Navarro, W. Hilber, A. Bonanni, and D. Stifter. Surface-stress-induced optical bulk anisotropy. *Physical Review B*, 62(19):13048, 2000. (Not cited.)
- [40] B. Hosten and M. Castaings. Transfer matrix of multilayered absorbing and anisotropic media. measurements and simulations of ultrasonic wave propagation through composite materials. *The Journal of the Acoustical Society of America*, 94(3):1488–1495, 1993. (Not cited.)
- [41] J. A. Huerta Ruelas et al. Anisotropias opticas en cristales de teluro de cadmio. *REPOSITORIO NACIONAL CONACYT*, 2009. (Not cited.)
- [42] I. Ionita. *Condensed matter optical spectroscopy: an illustrated introduction*. CRC Press, 2014. (Cited on page 18.)
- [43] I. G. Ivanov, J. U. Hassan, T. Iakimov, A. A. Zakharov, R. Yakimova, and E. Janzén. Layer-number determination in graphene on sic by reflectance mapping. *Carbon*, 77:492–500, 2014. (Not cited.)
- [44] A. Jorio, M. S. Dresselhaus, R. Saito, and G. Dresselhaus. *Raman spectroscopy in graphene related systems*. John Wiley & Sons, 2011. (Not cited.)
- [45] E. Kayhan. Graphene: Synthesis, characterization, properties and functional behavior as catalyst support and gas sensor. 2013. (Not cited.)
- [46] J. Kim and K.-B. Song. Recent progress of nano-technology with nsom. *Micron*, 38(4):409–426, 2007. (Cited on page 9.)
- [47] W. Y. Kim and K. S. Kim. Prediction of very large values of magnetoresistance in a graphene nanoribbon device. *Nature nanotechnology*, 3(7):408–412, 2008. (Not cited.)
- [48] G. Kucinskis, G. Bajars, and J. Kleperis. Graphene in lithium ion battery cathode materials: A review. *Journal of Power Sources*, 240:66–79, 2013. (Cited on page 5.)
- [49] A. H. Larsen, J. J. Mortensen, J. Blomqvist, I. E. Castelli, R. Christensen, M. Dułak, J. Friis, M. N. Groves, B. Hammer, C. Hargus, E. D. Hermes, P. C. Jennings, P. B. Jensen, J. Kermode, J. R. Kitchin, E. L. Kolsbjer, J. Kubal, K. Kaasbjer, S. Lysgaard, J. B. Maronsson, T. Maxson, T. Olsen, L. Pastewka, A. Peterson, C. Ros-tgaard, J. Schiøtz, O. Schütt, M. Strange, K. S. Thygesen, T. Vegge, L. Vilhelmsen, M. Walter, Z. Zeng, and K. W. Jacobsen. The atomic simulation environment—a python library for working with atoms. *Journal of Physics: Condensed Matter*, 29(27):273002, 2017. (Cited on pages VIII, 10, and 12.)

- [50] L. Lastras-Martínez, J. Almendarez-Rodríguez, G. Flores-Rangel, N. Ulloa-Castillo, O. Ruiz-Cigarrillo, C. Ibarra-Becerra, R. Castro-García, R. Balderas-Navarro, M. Oliveira Jr, and J. Lopes. Optical detection of graphene nanoribbons synthesized on stepped sic surfaces. *Journal of Applied Physics*, 122(3):035701, 2017. (Cited on pages 55 and 57.)
- [51] L. Lastras-Martínez, D. Medina-Escobedo, G. Flores-Rangel, R. Balderas-Navarro, O. Ruiz-Cigarrillo, R. Castro-García, M. d. P. Morales-Morelos, J. Ortega-Gallegos, and M. Losurdo. Differential reflectance contrast technique in near field limit: Application to graphene. *AIP Advances*, 9(4):045309, 2019. (Not cited.)
- [52] L. F. Lastras-Martínez, R. E. Balderas-Navarro, R. Castro-García, K. Hernández-Vidales, J. Almendarez-Rodríguez, R. Herrera-Jasso, A. Prinz, and I. Bergmair. Structural characterization of a capillary microfluidic chip using microreflectance. *Applied Spectroscopy*, 71(6):1357–1362, 2017. (Not cited.)
- [53] J. Li et al. Review of electrochemical capacitors based on carbon nanotubes and graphene. *Graphene*, 1(01):1, 2012. (Cited on page 5.)
- [54] T. S. Li, Y. C. Huang, S. Chang, Y. Chuang, and M.-F. Lin. Transport properties of ab-stacked bilayer graphene nanoribbons in an electric field. *The European Physical Journal B*, 64(1):73–80, 2008. (Not cited.)
- [55] S.-Y. Lin, N. T. T. Tran, S.-L. Chang, W.-P. Su, and M.-F. Lin. *Structure-and adatom-enriched essential properties of graphene nanoribbons*. CRC press, 2018. (Cited on page 8.)
- [56] J. Liu, R. Berger, K. Müllen, and X. Feng. Nanographenes and graphene nanoribbons with zigzag-edged structures. *From Polyphenylenes to Nanographenes and Graphene Nanoribbons*, pages 1–32, 2017. (Not cited.)
- [57] M. Losurdo and K. Hingerl. *Ellipsometry at the Nanoscale*. Springer, 2013. (Cited on page 20.)
- [58] H. Y. Mao, S. Laurent, W. Chen, O. Akhavan, M. Imani, A. A. Ashkarran, and M. Mahmoudi. Graphene: promises, facts, opportunities, and challenges in nanomedicine. *Chemical reviews*, 113(5):3407–3424, 2013. (Not cited.)
- [59] F. Mayinger. *Optical measurements: techniques and applications*. Springer Science & Business Media, 2013. (Not cited.)
- [60] J. Meyer-Holdt. *Experimental Methods for Implementing Graphene Contacts to Finite Bandgap Semiconductors*. PhD thesis, University of Copenhagen, Faculty of Science [Department of Nutrition . . .], 2016. (Not cited.)
- [61] P. Misra. *Applied Spectroscopy and the Science of nanomaterials*, volume 2. Springer, 2014. (Not cited.)

- [62] L. L. Missoni, G. P. Ortiz, M. L. M. Ricci, V. J. Toranzos, and W. L. Mochán. Rough 1d photonic crystals: A transfer matrix approach. *Optical Materials*, 109:110012, 2020. (Not cited.)
- [63] J. J. Mortensen, L. B. Hansen, and K. W. Jacobsen. Real-space grid implementation of the projector augmented wave method. *Phys. Rev. B*, 71:035109, Jan 2005. (Cited on pages 10 and 12.)
- [64] M. Mucha-Kruczyński. *Theory of Bilayer Graphene Spectroscopy*. Springer Science & Business Media, 2012. (Not cited.)
- [65] K. Müllen and X. Feng. *From Polyphenylenes to Nanographenes and Graphene Nanoribbons*, volume 278. Springer, 2017. (Cited on page 5.)
- [66] K. Nakada, M. Fujita, G. Dresselhaus, and M. S. Dresselhaus. Edge state in graphene ribbons: Nanometer size effect and edge shape dependence. *Physical Review B*, 54(24):17954, 1996. (Cited on page 8.)
- [67] Z. Ni, H. Wang, J. Kasim, H. Fan, T. Yu, Y. Wu, Y. Feng, and Z. Shen. Graphene thickness determination using reflection and contrast spectroscopy. *Nano letters*, 7(9):2758–2763, 2007. (Not cited.)
- [68] Z. H. Ni, T. Yu, Y. H. Lu, Y. Y. Wang, Y. P. Feng, and Z. X. Shen. Uniaxial strain on graphene: Raman spectroscopy study and band-gap opening. *ACS nano*, 2(11):2301–2305, 2008. (Cited on page 5.)
- [69] H. Nie, T. Shimizu, and H. Tokumoto. Atomic force microscopy study of pd clusters on graphite and mica. *Journal of Vacuum Science & Technology B: Microelectronics and Nanometer Structures Processing, Measurement, and Phenomena*, 12(3):1843–1846, 1994. (Cited on page 24.)
- [70] M. Oliveira Jr, T. Schumann, M. Ramsteiner, J. Lopes, and H. Riechert. Influence of the silicon carbide surface morphology on the epitaxial graphene formation. *Applied Physics Letters*, 99(11):111901, 2011. (Not cited.)
- [71] M. H. Oliveira Jr, J. M. J. Lopes, T. Schumann, L. A. Galves, M. Ramsteiner, K. Berlin, A. Trampert, and H. Riechert. Synthesis of quasi-free-standing bilayer graphene nanoribbons on sic surfaces. *Nature communications*, 6(1):1–7, 2015. (Not cited.)
- [72] D. Pandey, R. Reifenberger, and R. Piner. Scanning probe microscopy study of exfoliated oxidized graphene sheets. *Surface Science*, 602(9):1607–1613, 2008. (Not cited.)
- [73] A. M. Pinto, I. C. Goncalves, and F. D. Magalhaes. Graphene-based materials biocompatibility: a review. *Colloids and Surfaces B: Biointerfaces*, 111:188–202, 2013. (Cited on page 5.)

- [74] R. P. Prasankumar and A. J. Taylor. *Optical techniques for solid-state materials characterization*. CRC Press, 2016. (Not cited.)
- [75] C. A. Putman, K. O. Van der Werf, B. G. De Groot, N. F. Van Hulst, and J. Greve. Tapping mode atomic force microscopy in liquid. *Applied physics letters*, 64(18):2454–2456, 1994. (Cited on page 25.)
- [76] C. Rostgaard, J. J. Mortensen, and K. W. Jacobsen. Exact exchange in density functional calculations. *Master's thesis, Technical University of Denmark*, 2006. (Cited on pages 10 and 12.)
- [77] Y. R. Sapkota, A. Alkabsh, A. Walber, H. Samassekou, and D. Mazumdar. Optical evidence for blue shift in topological insulator bismuth selenide in the few-layer limit. *Applied Physics Letters*, 110(18):181901, 2017. (Not cited.)
- [78] L. Scholtz, L. Ladanyi, and J. Müllerová. Influence of surface roughness on optical characteristics of multilayer solar cells. 2014. (Not cited.)
- [79] F. Schwierz. Graphene transistors. *Nature nanotechnology*, 5(7):487, 2010. (Cited on page 5.)
- [80] Y. Shao, J. Wang, H. Wu, J. Liu, I. A. Aksay, and Y. Lin. Graphene based electrochemical sensors and biosensors: a review. *Electroanalysis: An International Journal Devoted to Fundamental and Practical Aspects of Electroanalysis*, 22(10):1027–1036, 2010. (Cited on page 5.)
- [81] E. Singh and H. S. Nalwa. Graphene-based bulk-heterojunction solar cells: a review. *Journal of nanoscience and nanotechnology*, 15(9):6237–6278, 2015. (Cited on page 5.)
- [82] A. Sivadasan. *Optical Properties of AlGaN Nanostructures*. PhD thesis, PhD thesis, Indira Gandhi Centre for Atomic Research Chennai, Tamil Nadu . . . , 2017. (Cited on pages X and 18.)
- [83] E. Sohmen, J. Fink, and W. Krätschmer. Electronic structure studies of undoped and n-type doped fullerene c60. *EPL (Europhysics Letters)*, 17(1):51, 1992. (Cited on page 8.)
- [84] Y.-W. Son, M. L. Cohen, and S. G. Louie. Energy gaps in graphene nanoribbons. *Phys. Rev. Lett.*, 97:216803, Nov 2006. (Cited on page 10.)
- [85] Y.-W. Son, M. L. Cohen, and S. G. Louie. Half-metallic graphene nanoribbons. *Nature*, 444(7117):347–349, 2006. (Cited on pages 8 and 9.)
- [86] M. Sprinkle, M. Ruan, Y. Hu, J. Hankinson, M. Rubio-Roy, B. Zhang, X. Wu, C. Berger, and W. A. De Heer. Scalable templated growth of graphene nanoribbons on sic. *Nature nanotechnology*, 5(10):727–731, 2010. (Cited on page 5.)

- [87] H. Tompkins and E. A. Irene. *Handbook of ellipsometry*. William Andrew, 2005. (Not cited.)
- [88] P. Török and F.-J. Kao. *Optical imaging and microscopy: techniques and advanced systems*, volume 87. Springer, 2007. (Not cited.)
- [89] D. Van Tuan. *Charge and spin transport in disordered graphene-based materials*. Springer, 2015. (Not cited.)
- [90] P. Vandenabeele. *Practical Raman spectroscopy: an introduction*. Wiley Online Library, 2013. (Not cited.)
- [91] J. R. Wallbank. *Electronic properties of graphene heterostructures with hexagonal crystals*. Springer, 2014. (Not cited.)
- [92] J. Weber, V. Calado, and M. Van De Sanden. Optical constants of graphene measured by spectroscopic ellipsometry. *Applied Physics Letters*, 97(9):091904, 2010. (Cited on page 20.)
- [93] U. Wurstbauer, C. Röling, U. Wurstbauer, W. Wegscheider, M. Vaupel, P. H. Thiesen, and D. Weiss. Imaging ellipsometry of graphene. *Applied Physics Letters*, 97(23):231901, 2010. (Not cited.)
- [94] G. Yang, C. Zhu, D. Du, J. Zhu, and Y. Lin. Graphene-like two-dimensional layered nanomaterials: applications in biosensors and nanomedicine. *Nanoscale*, 7(34):14217–14231, 2015. (Cited on page 5.)
- [95] G.-C. Yi. *Semiconductor nanostructures for optoelectronic devices: Processing, characterization and applications*. Springer Science & Business Media, 2012. (Cited on pages X and 18.)
- [96] L. Yu-Pu. Functionalization of two-dimensional nanomaterials based on graphene. (Not cited.)
- [97] A. Zangwill. density functional theory. *Physics today*, 68(7):34, 2015. (Cited on pages 10 and 12.)
- [98] B.-M. Zhang, M.-Y. Dong, and Z.-P. Qian. Incidence, reflection and transmission angles in anisotropic media. *Acta Seismologica Sinica*, 12(4):413–418, 1999. (Not cited.)
- [99] J. Z. Zhang. *Optical properties and spectroscopy of nanomaterials*. World Scientific, 2009. (Not cited.)
- [100] Q. Zhang, X. Li, M. M. Hossain, Y. Xue, J. Zhang, J. Song, J. Liu, M. D. Turner, S. Fan, Q. Bao, et al. Graphene surface plasmons at the near-infrared optical regime. *Scientific reports*, 4(1):1–6, 2014. (Not cited.)

- [101] Q. Zhong, D. Inniss, K. Kjoller, and V. Elings. Fractured polymer/silica fiber surface studied by tapping mode atomic force microscopy. *Surface Science Letters*, 290(1-2):L688–L692, 1993. (Cited on page 24.)
- [102] W.-R. Zhong, W.-H. Huang, X.-R. Deng, and B.-Q. Ai. Thermal rectification in thickness-asymmetric graphene nanoribbons. *Applied Physics Letters*, 99(19):193104, 2011. (Not cited.)
- [103] W. Zhu, C. Dimitrakopoulos, M. Freitag, and P. Avouris. Layer number determination and thickness-dependent properties of graphene grown on sic. *IEEE transactions on nanotechnology*, 10(5):1196–1201, 2011. (Not cited.)